IMMUNOLOGICAL ENTEROPATHY IN AN ACCELERATED MACAQUE MODEL OF AIDS

by
Joshua D. Croteau

A dissertation submitted to Johns Hopkins University in conformity with the requirements for the degree of Doctor of Philosophy

Baltimore, Maryland

November, 2016

ABSTRACT

Human immunodeficiency virus (HIV) infection is effectively controlled with combination antiretroviral therapy (cART). However, cART is insufficient to either purge HIV from the body or fully correct immunological imbalances acquired during acute infection. The gut contains the largest proportion of immunological cells in the body and is a primary target for initial and ongoing HIV replication in patients. cART patients exhibit alterations to memory T cell populations and develop gastrointestinal (GI) damage during infection. These are linked with microbial translocation, which is thought to be a primary source of inflammation in patients. Understanding the key cellular contributors to intestinal damage might provide insights into improving patient therapeutics and quality of life.

In this dissertation we examined whether or not a rapidly progressing SIV/pigtailed macaque model of HIV disease exhibits enteropathy, microbial translocation, and alterations to memory T cells populations similar to those seen in HIV-infected patients. Quantitative histological evaluation revealed that half of late stage infected (LSI) animals exhibited intestinal disease. Immunohistochemical staining combined with in situ hybridization revealed that intestinal disease was highly associated with T cell loss, increased cell death, increased numbers of SIV-infected cells, and decreased epithelial integrity. T cell numbers, epithelial integrity, and numbers of cytotoxic T lymphocytes were preserved in LSI animals without intestinal disease. Unexpectedly, measurement of plasma protein and DNA markers of microbial translocation revealed minimal evidence of microbial translocation.

Flow cytometry analysis showed a reduction in number of $CD4^+$ T cells in the blood and gut of LSI animals. cART initiated during acute infection restored $CD4^+$ T cells in the blood and colon and prevented intestinal disease. cART plus the CCR5 antagonist Maraviroc (cART+M) improved restoration of $CD4^+$ and $CD8^+$ memory T cell populations over cART alone. cART+M also markedly increased CD27 expression on memory T cells in all body regions indicating earlier differentiation of cells. Finally, markers of T cell activation were reduced in animals treated with cART+M. These findings provide unique insights into the status of the gut both physiologically and immunologically during HIV/SIV infection. Further, our findings with cART in combination with Maraviroc suggest a beneficial therapeutic opportunity for patients.

Thesis Advisor: Chris Zink

Thesis Reader: David Graham

ACKNOWLEDGEMENTS

I would like to express my appreciation for my mentor Dr. Chris Zink. You were always available to guide my scientific endeavors and give me support during occasional times of personal challenge. It was a truly rewarding experience to have a mentor whose disposition towards science and life was so in sync with my own. Despite undergoing changes in your career I always got the sense that you kept my education and training very high on your list of priorities and for that I'm thankful. Further, I appreciate the friendship you offered me as I evolved as a student and person; it made my experience during graduate school very enjoyable and personally rewarding. I would also like to thank my thesis committee members Dr. Joseph Mankowski, Dr. David Graham, and Dr. Alan Scott; you gave me critical feedback and guidance when I needed it most and aided me in evolving my science; I'm truly grateful to have been advised by such thoughtful scientists.

Thanks to all of the retrovirus lab members for tolerating my questions and requests year after year. Additionally, thanks for working alongside me for so long and generally making otherwise tedious work enjoyable. Special thanks to Elizabeth Engle and Erin Shirk for assisting in or conducting experiments for me countless times and giving me the privilege of your collaboration. Further thanks to Suzanne Queen, Brandon Bullock, Ming Li, and all of the other technicians I've had the privilege of working with in the retrovirus lab over the years. Thanks to my fellow graduate students and postdocs. Special thanks goes to Julia Drewes, Kelly Meulendyke, Jeanne Sisk, Dillon Muth, and Claudia Avalos for the

countless hours spent in the graduate student office providing sharp discussion, good stories, and camaraderie. Specifically to Julia and Kelly; thanks for allowing me to work alongside you on experiments even if they ran late into the night. These experiences gave me perspective on what it really means to be a committed scientist.

I also want to acknowledge and thank my fellow students, staff, and faculty in the Cellular and Molecular Medicine (CMM) graduate program. The mentorship, training, and friendship I gained through the CMM program was invaluable. As I enter the next stage of my career I know that I come adequately prepared and with a large network of friends and collaborators to support me in the future.

Finally, a huge thank you to my personal friends, family, and wife. To my friends who have been with me since high school or college, thank you for all of the support and good times we've experienced together. I can always depend on you to break me away from a difficult week or month and help me relax and let loose. To my parents: thank you for always believing in me even when I didn't believe in myself. Thank you for sticking with me through the chaotic time of my late teens and early twenties. And to my brother, thank you for giving me the privilege of watching you grow into a remarkable young man. To my wife, Brittany Croteau, there are not enough words I know to express my gratefulness for your love, support, positivity, and patience over the years. You've stuck with me since before I began this long journey to earning my doctorate and never once faltered

in your conviction that I can be successful in this path. Thank you for always giving me perspective and embracing the person I was and am becoming.

TABLE OF CONTENTS

LIST OF TABLES

Chapter II

LIST OF FIGURES

Chapter II

Chapter III

CHAPTER I.

Introduction

HIV, Inflammation, and Microbial Translocation

The modern era of human immunodeficiency virus (HIV) is defined by the achievement of combination antiretroviral therapy (cART) in suppressing viral replication in infected patients. This suppression has led to individuals living longer, healthier lives (1). Despite the success of cART, it is insufficient to either purge the latent reservoir of virus-infected cells or fully correct the immunological imbalances acquired during acute HIV infection (2, 3). In the plasma of patients on cART there is ongoing evidence of low-level viral replication (4, 5). In chronically infected individuals, there is ongoing indication of systemic inflammation in the plasma along with an increased risk for non AIDS-related events such as cardiovascular, hepatic, and renal diseases (6). Risk factors for these non-AIDS events include elevated C-reactive protein (CRP), D-Dimer, IL-6, and hyaluronic acid (7). These inflammatory markers do not resolve even with suppression of viral replication by cART (8). One of the main triggers for this systemic inflammation is thought to be increased microbial translocation due to an impaired mucosal immune system and resulting intestinal damage, which does not resolve with cART (9). This translocation along with the amount of CD4+ T cell recovery after cART implementation predict HIV disease progression and the overall prognosis of patients (10-12).

Natural controllers of HIV replication have much more complete restoration of CD4+ T cell populations in the blood, which coincides with control of viral replication. However, these individuals do not experience a reduction in some indicators of systemic inflammation, which coincide with non AIDS events

such as cardiac disease (13). Additionally, in some cohorts of controllers, indicators of microbial translocation such as lipopolysaccharide are elevated compared to uninfected individuals and are associated with loss of viral control (14). These observations that persist even in the presence of natural viral suppression and effective cART drivers of systemic inflammation have driven researchers to define the immunological parameters that frame these events. Better understanding of these immunological players should shed light on changes independent of viral replication that contribute to persistent inflammation.

HIV-Associated Intestinal Dysfunction and Immunological Impairment

Since the beginning of the AIDS epidemic, gastrointestinal (GI) complications have been noted by clinicians. Over half of all HIV-infected patients suffer from symptoms such as pain and diarrhea. Additionally, nearly all patients on long term cART therapy exhibit GI complications at some point (15). These GI manifestations are multifaceted and might include gastritis, enteritis, and upper and/or lower GI opportunistic infections with viral, microbial, and protozoal organisms (16). Evaluation of clinical hematoxylin and eosin (H&E)-stained intestinal sections by a pathologist is sufficient to make a diagnosis of HIV-associated GI disease. More detailed differential diagnoses might be made that implicate specific pathogens contributing to overall disease using a variety of

techniques such as polymerase chain reaction (PCR), immunohistochemistry (IHC), and in situ hybridization (ISH) (17).

Enteropathy observed in HIV-infected individuals, with and without cART, is a consequence of complex and devastating immunological imbalances triggered by HIV replication. Since the late 1980s it has been noted that CD4+ T cells are rapidly and dramatically lost in the GI tract, specifically the jejunum, of acutely and chronically HIV-infected individuals (18, 19). These T cell populations do not recover upon implementation of cART (20-22). In models of HIV disease similar findings have been observed with regards to GI disease, depletion of CD4+ T cells, and subsequent inadequate recovery after initiation of cART (23-28). These reductions in the number of CD4+ T cells in the intestinal mucosa specifically involve alterations in the numbers of and activation state of specialized lineages of T cells including central and effector memory cells, intermediately differentiated memory cells, Th17 cells, and T regulatory cells in both humans and SIV infected primates. Alterations to the balance of these specialized T cells result in reduced production of the proliferative cytokine interleukin 2 (IL-2) and increased production of pro-inflammatory cytokines such as macrophage inflammatory protein 1β (MIP-1β) and interferon gamma (IFNγ). Overall, these changes contribute to a maladaptive mucosal immune system that leads to increased local inflammation (29-37).

Macrophages are a large constituent of the gut and are typically of an anti-inflammatory phenotype. Macrophages of the gut normally function to eliminate cellular debris from the local microenvironment. They're largely localized to the

basolateral surface of the epithelium and are constantly receiving anti-inflammatory signals from the surrounding lamina propria (38-40). During acute and chronic HIV infection they are infected, yet reportedly they persist and even accumulate concurrently with the loss of CD4+ T cells (38). During chronic HIV infection and in patients receiving cART, their phenotype shifts to a pro-inflammatory state. This results in increased expression of pro-inflammatory cytokines such as tumor necrosis factor alpha (TNFα), IFNγ, and interleukin 1b (IL1β) (39-43). This shift in macrophage and T cell cytokine expression along with the loss of specialized T cell populations are the foundation of immunological dysfunction during HIV/SIV infection of the gut mucosa; leading to disruption of normal GI function and the ability of the tissue to respond to pathogens, clear cellular debris, and control inflammation.

The Challenges of Studying Microbial Translocation

HIV and SIV associated immunological impairment of the mucosal immune system is generally associated with breakdown of the mucosal barrier ultimately resulting in increased microbial translocation both during acute and chronic HIV infection, and with cART (12, 36, 41-45). There are several indicators of microbial translocation used to measure the amount of translocation occurring. These include but are not limited to: lipopolysaccharide (LPS), soluble CD14 (sCD14), LPS binding protein (LBP), and 16s ribosomal DNA (16s rDNA). These various assays have been used to predict both disease outcome as well

as the amount of immunological restoration HIV-infected patients on cART undergo with varying degrees of success (46-49). Further, some groups have reported methodological limitations of several of these assays; highlighting the need for thorough and rigorous evaluation of translocation using several approaches (46, 50, 51).

Project Overview

As previously discussed, there is strong evidence that HIV/SIV-associated disruption of the gut mucosal immune system is central to the ongoing inflammation experienced by chronically HIV-infected patients and those on cART. Given the complex physiology and immunology of the GI tract, approaches that attempt to evaluate the severity of HIV/SIV associated enteropathy, define its immunological basis, and potentially associate findings with increased microbial translocation and inflammation need to be rigorous and thorough. While there is evidence of microbial translocation and a body of research indicating its importance in driving HIV/SIV disease, rarely do studies seek to evaluate intestinal pathology alongside immunological changes and microbial translocation. Approaches that include detailed examination of specific aspects of disease in combination with those that seek to broadly evaluate many aspects of disease in a single system might help to clarify some confusion regarding the topic. Additionally, these findings might reveal potential

opportunities for improved therapeutics by highlighting the most potent drivers of inflammation in the gut and systemically.

While enteropathy has been described in HIV-infected humans and some SIV models of HIV infection, it has not been examined in the accelerated SIV/macaque dual inoculation model of HIV. This model exhibits a course of disease similar to SIV-infected rhesus macaques but in a compressed time span resulting in death around three months post inoculation, and infected animals can achieve viral suppression on cART therapy (52). This model has previously provided unique insights into various aspects of the disease that develop longitudinally in the host, such as HIV-associated neurocognitive disease (HAND). Further, this model has served as a system to test novel neurological and systemic therapeutics (53-56).

The aim of this dissertation was to examine whether or not this rapidly progressing SIV/pigtailed macaque model of HIV disease exhibits enteropathy, microbial translocation, and alterations to memory T cells populations similar to those seen in HIV-infected patients. In Chapter II we show that intestinal disease develops in half of infected macaques during late stage infection (LSI), and is prevented by cART initiated during acute infection. This intestinal disease was most severe in the ileum and colon, and as such we chose these two regions for further analysis. In the ileum and colon, intestinal disease was associated with increased cellular apoptosis via caspase-3 staining, decreased staining for CD3+ T cells via immunohistochemistry (IHC), and an increased number of SIV-infected cells via *in situ* hybridization (ISH). In LSI animals that did not develop

intestinal disease, CD3+ T cells were preserved. Further, for all LSI animals, levels of CD3 staining in the gut mucosa strongly correlated with the number of infected cells in the gut mucosa, plasma viral load, and caspase-3 staining. Surprisingly, there was little evidence of microbial translocation in the plasma as measured by soluble CD14, soluble CD163, lipopolysaccharide binding protein; or in the plasma, mesenteric lymph nodes, and liver as measured by microbial 16s ribosomal DNA. To explore this finding further, we examined ileum and colon samples from animals during acute and asymptomatic infection for loss of epithelial integrity indicated by loss of staining for the tight junction protein claudin-3. Claudin-3 loss was not observed during acute infection despite significantly less staining for CD3+ T cells. However, claudin-3 was reduced in LSI animals with severe intestinal disease although this did not predict increased microbial translocation. LSI animals that did not develop intestinal disease had increased TIA-1-positive cytotoxic T lymphocytes (CTLs) suggesting a robust, adaptive, CTL response might, in part, confer resilience to SIV induced intestinal damage. Thus, in this accelerated SIV macaque model, microbial translocation occurs during late stage infection and might be associated with an alternative pathway to microbial antigen induction independent of intestinal disease and epithelial damage.

In Chapter III of this dissertation we conduct a detailed analysis of naive, central, and effector memory T cells, and their expression of CD27, CCR5, CCR7, and HLA-DR in the blood, gut mucosa (jejunum, ileum, and colon), and draining gut and peripheral lymph nodes of uninfected animals in comparison

with those during late stage infection (LSI); and animals receiving cART, and cART plus Maraviroc (cART+M) using multicolor flow cytometry. The numbers of CD4+ T cells were lower in the blood and in all areas of the gut mucosa of LSI animals. These reductions were restored with cART in the blood, ileum, and colon; and with cART+M in the blood and colon. cART+M improved restoration of CD4+ and CD8+ naive and central memory T cells towards proportions seen in uninfected animals as compared to cART alone in the gut mucosa. cART+M also markedly increased CD27 expression on naïve, central, and effector CD4+ memory T cells in all body regions, and on central, and effector CD8+ memory T cells in the ileum and colon. Increased CD27 expression indicates the cells are less terminally differentiated and as such are more able to respond effectively and appropriately to inflammatory stimuli. Finally, reductions were observed in CCR7 in the blood and HLA-DR in the gut mucosa on CD4+ and CD8+ memory T cells indicating a reduction in activation of T cells. Overall, these findings indicate that while cART might be effective at preventing the development of intestinal disease as evaluated by histopathology, therapeutic regimens can be further improved to yield additional restoration of the mucosal immune system. Additionally, we identify a drug already in use for HIV therapy, the CCR5 receptor antagonist Maraviroc, that is capable of restoring the proportions of memory T cells in infected animals towards those seen in uninfected animals while reducing their exhaustion and activation; indicating an overall reduction in inflammation.

CHAPTER II.

Marked Enteropathy in an Accelerated Macaque Model of AIDS

This Chapter has been accepted for publication in the *American Journal of Pathology*

Abstract

Enteropathy in human immunodeficiency virus (HIV) infection is not eliminated with combination antiretroviral therapy (cART), and is possibly linked to microbial translocation. We used a rapidly progressing SIV/pigtailed macaque model of HIV to examine enteropathy and microbial translocation. Histological evidence of intestinal disease was observed in only half of infected macaques during late stage infection (LSI). cART initiated during acute infection prevented intestinal disease. In the ileum and colon, enteropathy was associated with increased caspase-3 staining, decreased CD3+ T cells, and increased SIV-infected cells. CD3+ T cells were preserved in LSI animals without intestinal disease and levels of CD3 staining in all LSI animals strongly correlated with the number of infected cells in the intestine and plasma viral load. Unexpectedly, there was little evidence of microbial translocation as measured by soluble CD14, soluble CD163, lipopolysaccharide binding protein, and microbial 16s ribosomal DNA. Loss of epithelial integrity indicated by loss of the tight junction protein claudin-3 was not observed during acute infection despite significantly fewer T cells. Claudin-3 was reduced in LSI animals with severe intestinal disease but did not correlate with increased microbial translocation. LSI animals that did not develop intestinal disease had increased TIA-1 positive cytotoxic T lymphocytes (CTLs) suggesting a robust adaptive CTL response might, in part, confer resilience to SIV induced intestinal damage.

Introduction

With the implementation of combination antiretroviral therapy (cART) human immunodeficiency virus (HIV)-infected people are living longer, healthier lives. The number and median age of people living with HIV has increased rapidly since the pre cART era with over 37 million individuals infected worldwide (1). As this population grows and ages, management of chronic HIV-associated conditions is becoming of increasing importance in the health community.

Over half of all HIV-infected patients suffer from gastrointestinal (GI) symptoms such as pain and diarrhea. Additionally, nearly all patients on long term cART therapy exhibit GI complications at some point (2). These complications have been evident since the beginning of the AIDS epidemic and are often multifaceted including gastritis, enteropathy, and upper and/or lower GI opportunistic infection with viral, microbial, and protozoal organisms (3). Visual evaluation of hematoxylin and eosin (H&E) stained intestinal sections is sufficient to make a diagnosis of HIV-associated GI disease. Additionally, differential diagnoses might be made implicating specific pathogens contributing to overall disease using a variety of techniques such as polymerase chain reaction (PCR), immunohistochemistry (IHC), and in situ hybridization (ISH) (4).

The pathological changes that occur in the gut of HIV-infected individuals, both cART treated and untreated, are thought to result from complex HIV-induced immunological changes. CD4+ T cells are rapidly and dramatically decreased in the GI tract of acutely and chronically HIV-infected individuals and

are often reported to recover incompletely with implementation of cART (5, 6). Some specialized lineages of T cells including Th17 cells and T regulatory cells are affected by this loss contributing to the inflammatory imbalance (7). Macrophages, which are a large constituent of the gut and typically of an anti-inflammatory profile, are infected early on. However, they persist and even accumulate concurrently with the loss of CD4+ T cells (8, 9). Dendritic cells, which assume an antigen-presenting role in the gut, are rapidly lost with infection, and are replaced by pro-inflammatory pDCs even in patients on cART (10). These overall shifts in immunological cell populations disrupt normal GI function as well as the ability of the tissue to respond to pathogens, clear cellular debris, and control inflammation.

As studying the nature of HIV-associated GI disease in patients is experimentally challenging, non-human primate (NHP) models of HIV using simian immunodeficiency virus (SIV) provide a unique window of insight into the course of this disease. Exhibiting a similar course of disease both virologically and immunologically, many of these models have been reported to have pathological changes in the gut and significant alterations in the gut-associated lymphoid tissue (GALT) that are similar to humans with HIV (11, 12).

In both HIV-infected humans and SIV-infected NHPs the intestinal disease caused by immunological dysfunction is thought to result in disruption of the gut barrier. This disruption might be sufficient to allow translocation of microbial products and microbes themselves into the lymphatic system and blood stream. This translocation, which is thought to be a main source of systemic inflammation

and ultimately an important component of terminal opportunistic infection, is not wholly restored with cART treatment in either humans or NHPs (13-15).

Additionally, recent advances in the study of the microbiota in human health and disease have expanded our understanding of the role of the gut during disease progression. Shifts in the microbiome been associated with disease outcome in humans and have provided insights into potential mechanisms associated with cART therapy and even protection conferred from experimental vaccine approaches (16, 17).

While enteropathy has been identified and evaluated in HIV-infected humans and some NHP models of HIV infection, it has not been examined in the accelerated SIV/macaque dual inoculation model of HIV (18). Briefly, this model exhibits a course of disease similar to SIV-infected rhesus macaques but in a compressed time span resulting in death around three months post inoculation, and infected animals can achieve viral suppression on cART therapy. This model has previously provided unique insights into various aspects of the disease that develop longitudinally in the host, including HIV-associated neurocognitive disease (HAND) (19). The aim of the present study was to evaluate the presence and severity of intestinal disease and its association with viral infection and/or alterations to cell populations in the GI tract of SIV dual virus-inoculated macaques. Specifically, changes to peripheral and GI viral burden, blood CD4+ T cell count, GI apoptosis, GI T cells and macrophages, intestinal tight junction continuity, indicators of microbial translocation, and translocation associated inflammation were evaluated.

Materials and Methods

Animal studies

Tissues from multiple cohorts of juvenile pigtailed macaques were studied retrospectively. All infected groups were inoculated intravenously with two strains of SIV, the immunosuppressive swarm SIV/DeltaB670 and the neurovirulent clone SIV/17E-Fr, as previously described (17). Infected, untreated animals were euthanized during various stages of disease (7, 10, 14, 21, 35, 42, 56, and approximately 84 days p.i.). Animals that were euthanized at 84 days or prior to that time if criteria for euthanasia were reached are herein referred to as late stage infection (LSI).

Animals referred to as “cART” received a regimen including the nucleotide reverse-transcriptase inhibitor tenofovir (Gilead, Foster City, CA) at a dose of 30 mg/kg subcutaneously once a day from days 12 to 26 p.i. and 10 mg/kg subcutaneously once a day thereafter; the protease inhibitors saquinavir (Roche, Basel, Switzerland) and atazanavir (Bristol-Myers Squibb, New York City, NY) at doses of 205 and 270 mg/kg orally twice a day, respectively; and the integrase inhibitor L-870812 (Merck, Kenilworth, NJ) at a dose of 10 mg/kg orally twice a day beginning at 12 days after virus inoculation. cART animals were monitored for virus in plasma and CSF by quantitative real-time PCR (qRT-PCR) and experienced marked declines in plasma and CSF viral RNA levels, reaching <100 copy equivalents/mL by ~50 days after treatment initiation. cART animals were euthanized between 161-175 days post infection and have been described

in further detail previously (20). Animals referred to as procedural control (PC) were mock-infected and had blood sampled on the same experimental schedule as untreated late stage SIV-infected (LSI) animals. PC animals were euthanized at 84 days p.i. Animal groups evaluated in this study are summarized in Table 1-1.

All animals were euthanized in accordance with federal guidelines and institutional policies. At euthanasia animals were anesthetized with ketamine-HCl followed by induction of deep anesthesia with pentobarbital and perfused with sterile PBS. Tissues were collected and either flash frozen or fixed with Streck tissue fixative (Streck, La Vista, NE) for subsequent use. All animal studies were approved by the Johns Hopkins Animal Care and Use Committee; all animals were humanely treated in accordance with federal guidelines and institutional policies.

Histological scoring for intestinal disease

Following necropsy, tissues were fixed using Streck tissue fixative for one week at room temperature and then embedded in paraffin. Sections of the stomach, duodenum, jejunum, ileum, cecum, and colon were prepared and stained with hematoxylin and eosin. A semiquantitative scoring template was established in consultation with a board certified veterinary pathologist to evaluate several visual indicators of intestinal disease. The presence of mixed mononuclear cellular infiltrates, multinucleated giant cells, and parasites, were

qualitatively assigned a score of 0 (none), 1 (mild), 2 (moderate), or 3 (severe). Thickness and integrity of the epithelium was examined and assigned a score of 0 (intact), 2 (possibly compromised), or 4 (markedly compromised). Villus and glandular fusion, loss, abscesses, dilation, lymphoid follicles, and submucosal mononuclear cells were individually assigned a score of 0 (absent), or 1 (present). The sum of these scores was used as a measure of severity of intestinal disease in each section. The sum of all of the scores for each section was used to assign a severity score for each animal.

To quantitate severity of intestinal disease, sections were blinded and systematically examined under light microscopy by a single investigator. A separate pathologist evaluated and scored all sections from 24 animals to control for observer bias. Each scoring criterion was individually correlated with total scores to ensure one criterion was not influencing overall results. No PC or cART animal had an intestinal disease score above the median score (27) for LSI animals. As a result, this number was used to define animals with and without intestinal disease. Animals with scores between the 50th and 75th percentile (27-32) were said to have mild intestinal disease, animals with scores above the 75th percentile (33+) were said to have severe intestinal disease.

Immunohistochemistry and in situ hybridization

Double labeling of tissues using immunohistochemistry (IHC) and in situ hybridization (ISH) was performed by hand on fixed, paraffin-embedded tissue

sections. Sections were deparaffinized by baking at 60°C, then rehydrated through a graded alcohol series. Slides were then pretreated with 25 µg/mL of proteinase K (Roche Applied Science, Indianapolis, IN). In situ hybridization for SIV was performed using an antisense SIVmac239 digoxigenin-UTP-labeled riboprobe at a concentration of 1.75 ng/µL overnight at 51°C. After washing, anti-digoxigenin antibody was applied for 1 h at 37°C followed by the addition of color substrate solution to slides overnight at 4°C. Uninfected tissues were used as controls. After washing, slides were then blocked with 1x Power Block (BioGenex) for 10 min before proceeding to immunohistochemistry.

Secondary labeling for macrophages was accomplished by using a monoclonal antibody against CD68 (KP1, Dako, Glostrup, Denmark) at a concentration of 74 µg/L for 60 min at RT. Secondary labeling for T cells was accomplished using a polyclonal antibody against CD3 (A0452, Dako) at a concentration of 60 µg/mL for 60 min at RT. After washing, biotinylated secondary antibody was added for 30 min following which slides were washed and visualized using the Vector red alkaline phosphatase substrate kit (Vector Laboratories, Burlingame, CA). After staining, slides were washed, dehydrated and cover-slipped.

Apoptosis was measured on tissue in the absence of ISH using a rabbit polyclonal antibody against caspase-3 (9661, Cell Signaling, Danvers, MA) at a concentration of 0.252 µg/mL for 15 min at room temperature. All caspase-3 staining was conducted on the Leica Bond Rx automated tissue staining system

using the Leica Bond Polymer Refine staining kit using a 20 minute sodium citrate pretreatment.

Epithelial tight junction protein claudin-3 was measured on tissue in the absence of ISH using a rabbit polyclonal antibody against claudin-3 (RB-9251, ThermoFisher, Waltham, MA) at a concentration of 4 μg/mL for 15 min at room temperate. All claudin-3 staining was conducted on the Leica Bond Rx automated tissue staining system using the Leica Bond Polymer Refine staining kit using a 20 minute sodium citrate pretreatment.

Cytotoxic T lymphocytes were measured in tissue in the absence of ISH using a mouse monoclonal antibody against TIA1 (T-cell intracytoplasmic antigen) antibody at a concentration of 10 μg/mL for 15 min at room temperature. All TIA-1 staining was conducted on the Leica Bond Rx automated tissue staining system using the Leica Bond Polymer Refine Red staining kit using a 30 minute sodium citrate pretreatment.

All tissue sections were evaluated and quantified using a Nikon Eclipse microscope fitted with a color Nikon DS-Ri1 camera and NIS Elements Acquisition and Analysis software (Version 3.22.00, Nikon, Tokyo, Japan). Slides were blinded and 4 x 4 to 8 x 8 grids of adjacent microscope fields were imaged at 200x power resulting in a composite image containing at least 16 microscopic fields. Composite images were then white balanced and background corrected. Quantitation for CD3, CD8, and caspase-3 was accomplished by defining regions of interest (ROI) manually between the muscularis mucosae and the gut lumen

including the epithelium. Peyer's patches and lymphoid follicles were excluded due to their variability in numbers and location in the ileum and colon. ROIs were limited to those where the crypts/glands were in the same plane as the histological section. Several regions of interest were defined resulting a total of approximately 2 mm2 of mucosa analyzed. ROIs were analyzed for immunohistochemically positive cells using the same object count settings for each marker between all blinded samples resulting in both a percentage of ROI area (% ROI) and number of positive cells. The same ROIs on each slide were then manually scored for SIV-ISH-positive cells yielding a number of positive cells per ROI and a ratio of singly ISH-positive cells to those double positive for ISH and IHC.

Percent loss of claudin-3 staining was calculated in an approach similar to that detailed by Estes et al (14). Briefly, the luminal surface of the epithelium was traced and measured on composite images of the gut lamina propria resulting in a boundary at least 1mm in length. Then, all stretches of the epithelium lacking claudin-3 staining were traced and measured. The sum of the lengths of epithelium lacking claudin-3 staining were divided by the overall length of the epithelium and multiplied by 100 to yield a percent loss of claudin-3.

The number of cells positive for TIA-1 was evaluated by counting the total number of TIA-1 positive cells in three microscope fields where the crypts/glands were in the same plane as the histological section at 400 x magnification. The mean of these three counts was then calculated resulting in an average TIA-1 positive cells number per field.

RNA extraction and qRT-PCR of SIV in plasma

Viral RNA was isolated from 400 mL of plasma collected terminally using the QIAamp MiniElute Virus Spin kit (Qiagen, Hilden, Germany). Samples were eluted in 40 μL of Tris and ethylenediaminetetraacetic acid buffer and analyzed in triplicate by quantitative realtime PCR, as described elsewhere (19). The limit of detection for the assay was established as 10 copies/reaction (100 copy equivalents/mL).

CD4+ T cell count

Terminal blood CD4+ T cell count was obtained by evaluating total number of lymphocytes per mL of blood via CBC. Then, using multicolor FACS analysis, an absolute percentage of lymphocytes positive for CD4 was determined. This percentage was then multiplied by the absolute number of lymphocytes per mL of blood to determine the number of CD4 cells per mL blood. This method has been described in detail elsewhere. (22)

DNA extraction and 16s rDNA qPCR in plasma and tissues

DNA was extracted from 200 μL previously thawed plasma using the QIAmp DNA Mini kit (51304, Qiagen). DNA from liver and MLN was extracted from approximately 50 mg of disrupted frozen tissue using the DNeasy kit

(69504, Qiagen). Real time PCR results were obtained using the Microbial DNA qPCR Pan Bacteria 1 assay (Qiagen) on a CFX96 thermocycler (Biorad, Hercules, CA). A 16s rDNA standard was established using DNA from 1 mL of an overnight E. coli K12 (ER2925, NEB) culture. DNA was extracted from the E. coli cell pellet using the QIAmp DNA Mini kit (51304, Qiagen). DNA purity and concentration was measured using a Nanodrop spectrophotometer (ND-1000, BioRad). After determining the DNA concentration the number of genome equivalents was calculated using the known E. coli K12 genome size. A 1:15 8-fold dilution series was then used to establish a standard curve down to <1 genome per reaction. Limit of detection was established at <30 E. coli K12 genome equivalents per reaction.

Plasma sCD14, s163, & LBP

sCD14 was measured via sandwich ELISA on 100 µL thawed plasma in 1:200 dilution using the human sCD14 Quantikine ELISA kit (R&D Systems, Minneapolis, MN). sCD163 was measured via sandwich ELISA on 50 µL undiluted thawed monkey plasma using the human sCD163 Quantikine ELISA kit (R&D Systems). LPS binding protein (LBP) was measured in 100 µL undiluted thawed monkey plasma using the human LBP ELISA kit (Abnova, Taipei City, Taiwan). All plates were analyzed using an iMarkTM microplate reader (Biorad).

Statistical analyses

Comparisons between two treatment groups were done using Mann-Whitney tests. Comparisons between multiple treatment groups were done using Kruskal-Wallis tests followed by Dunn's multiple comparisons tests between the mean ranks of every group. Correlations were determined using Spearman's rank correlation tests, or Pearson's correlation tests. *p* values for multiple correlations were corrected using Benjamini Hochberg multiple comparisons correction. Microsoft excel 2013 was used to organize data and generate descriptive statistics. GraphPad Prism 6.0 was used to perform all other statistical analyses and generate graphs. Graphs showing Kruskal-Wallis group comparisons report *p* values after Dunn's corrections.

Results

Intestinal disease scoring criteria

To evaluate the impact of each intestinal disease scoring criteria on the total score, the criteria were broken down into four main categories; giant cells, cellular infiltrates, epithelium integrity, and villus/gland disruption. The descriptive statistics for LSI and PC animals were compared and the average scores for each disease indicator category compared (Table 1-2). LSI animals scored higher in all categories than PC animals. Multinucleated giant cells were not observed in PC animals but were seen in 58.3% of LSI animals. Mixed cellular infiltrates were observed in all animals as some density of lymphocytes and macrophages are normal in the lamina propria of the gut. The epithelium was compromised in 29.1% more LSI animals than PC animals. Abnormal villi and glands were only observed in 8.3% of PC animals but were observed in 66.7% of LSI animals.

Pearson's correlation tests were carried out between each of the four categories (giant cells, cellular infiltrates, epithelium integrity, and villus/glad disruption) and the overall intestinal disease score for LSI animals. All four categories significantly correlated with the overall intestinal disease score. However, none of the correlations was especially strong. Of the categories, villus and glandular abnormalities were the best predictors of total intestinal disease severity ($r = 0.50$, $r2 = 0.25$, $p < 0.0001$). Cellular infiltrates were the worst predictors of total intestinal disease severity ($r = 0.26$, $r2 = 0.07$, $p < 0.0001$).

Detailed evaluation of the intestinal severity scoring criteria both total and by anatomical location are described in Supplemental tables 1-1, 1-2, and 1-3.

Intestinal disease scores

The first goal was to unbiasedly characterize the nature of any observable histopathological changes in several cohorts of SIV-infected macaques. These groups included: uninfected procedural control animals (PC), infected animals euthanized at various stages of infection, and infected animals treated with combination antiretroviral therapy (cART) starting at day 12 post inoculation. Information on animal groups is summarized in Table 1-1.

Tissues from each animal were evaluated for indicators of intestinal disease using a scoring system detailed in the methods section. Briefly, changes such as mixed cellular infiltration, villus and glandular disruption, presence and overgrowth of microflora, and disruption of the epithelium were evaluated and individually assigned scores; the sum of which indicated that GI region's severity of intestinal disease. The sum of the scores for all regions of the gastrointestinal tract represented each animal's overall intestinal disease score. Representative images of normal animals, and animals with several of these disease indicators are depicted in Figure 1-1 A-F.

There was a significant difference in the mean rank between all of the animal groups examined (Figure 1-1G; $H = 22.73$, $p < 0.0001$). Specifically, late state infected (LSI) animals exhibited significantly more intestinal disease than

matched procedural control (PC) animals ($p = 0.0002$) (Figure 1-1H). Interestingly, animals that received combination antiretroviral therapy (cART) had levels of intestinal disease that were significantly lower than LSI animals and were similar to PC animals ($p = 0.0129$) (Figure 1-1H). Of the other time points examined, only two animals euthanized at day 56 post-infection had scores above 27; both of these had mild enteropathy (Figure 1-1G).

Relationship between intestinal disease, plasma viral load, and blood CD4+ T cell count

Severity of intestinal disease was compared with terminal plasma viral load (pVL) and terminal blood CD4+ T cell count for all LSI animals, both with and without enteropathy. There was no overall correlation with all LSI animals. However, when animals with mild or severe intestinal disease were examined separately, there was a highly significant positive correlation between plasma viral load and the severity of intestinal disease ($r = 0.841$, $p = 0.0006$) (Figure 1-1I). Additionally, in animals with severe intestinal disease there was a significant negative correlation between terminal blood CD4 count and severity of intestinal disease ($r = -0.9710$, $p = 0.011$) (Figure 1-1J).

Intestinal disease by intestinal region

With the exception of the duodenum, all intestinal sites examined trended towards or had significantly different mean ranks of intestinal disease between PC, cART, and LSI animals (Figure 1-2A-F). The strongest statistical differences in mean rank of intestinal disease were found in the ileum ($H = 16.51$, $p = 0.0003$) and colon ($H = 23.00$, $p < 0.0001$) (Figure 1-2D, F). All group differences represented a significant increase or trend towards an increase in the mean rank of intestinal disease in LSI animals. The most significant elevations in mean rank of intestinal disease between PC and LSI animals were in the ileum ($p = 0.0025$) and colon ($p < 0.0001$). With these findings, we selected the ileum and colon for subsequent study.

Caspase-3 expression in ileum and colon

Caspase-3 expression was measured using immunohistochemistry (IHC) to evaluate the levels and locations of apoptosis in the ileum and colon of PC animals compared with LSI animals with or without severe intestinal disease (LSI-Severe or LSI-None). In PC animals, caspase-3 was concentrated in proximity to the gut lumen; the tips of the villi in the ileum and the superficial lamina propria of the colon (Figure 1-3A, B). However, in LSI-Severe animals, caspase-3 localized around areas of villus loss in the ileum and glandular degeneration in the colon (Figure 1-3C, D). There was a significant difference in the mean rank of percent region of interest (% ROI) positive for caspase-3 between PC, LSI-None, and LSI-Severe animals in the ileum ($H = 8.769$, $p =$

0.0012) and colon (H = 5.692, p = 0.0487) (Figure 1-4A, B). The % ROI positive for caspase-3 was found to be significantly increased in LSI-Severe animals as compared with PC animals in the ileum (p = 0.0098) and trended towards an increase between LSI-None and LSI-Severe animals in the colon (p = 0.0930).

CD3 expression and distribution in the ileum and colon

Slides from the ileum and colon of PC animals, LSI-None, and LSI-Severe animals were dually labeled for CD3 and SIV using IHC and in situ hybridization (ISH). In PC animals, CD3 positive cells were distributed evenly throughout the lamina propria in the ileum and colon (Figure 1-3E, F). However, in LSI-Severe animals, what CD3 positive cells remained congregated in foci located around the muscularis mucosae (Figure 1-3G, H). There was a significant difference in the mean rank of the % ROI positive for CD3 between PC, LSI-None, and LSI-Severe animals in the ileum (H = 7.269, p = 0.0152) and colon (H = 7.538, p = 0.0107) (Figure 1-4C, D). These group differences represented a significant decrease between the mean rank of the % ROI positive for CD3 between LSI-None and LSI-Severe animals in the ileum (p = 0.0243) and colon (p = 0.0324). Additionally, while only approaching significance, CD3 % ROI tended to be significantly lower between PC and LSI-Severe animals in the colon (p = 0.0930).

CD68 expression and distribution in ileum and colon

Slides from the ileum and colon of PC, LSI-None, and LSI-Severe animals were also dually labeled for CD68 and SIV using IHC and ISH respectively. In PC animals, CD68-positive cells were concentrated in proximity to the gut lumen: the tips of the villi in the ileum and near the basal surface of the colon epithelium (Figure 1-3I, J). However, in LSI-Severe animals, CD68-postive cells were evenly distributed throughout the lamina propria in the ileum and concentrated around degenerating glands in the colon (Figure 1-3K, L). In the colon there was a significant difference in mean rank of the % ROI positive for CD68 between PC, LSI-None, and LSI-Severe animals ($H = 5.808$, $p = 0.0442$) (Figure 1-4E, F). This represented a significant reduction in CD68 between PC animals and LSI-Severe animals ($p = 0.0482$). No differences in mean rank of the % ROI positive for CD68 in the ileum were found.

SIV hybridization and double labeled cells in ileum and colon during late stage infection

Slides double-labeled for CD3/SIV or CD68/SIV were scored for number of cells that were positive for SIV RNA alone or double-labeled for SIV and CD68. Overall, the number of SIV-positive cells was significantly higher in the ileum but not in the colon of LSI-none as compared with LSI-Severe animals ($p = 0.0286$) (Figure 1-5A). The total number of CD3/SIV or CD68/SIV double positive cells was not significantly different in the ileum or colon of LSI-None and LSI-

Severe animals. However, CD68/SIV represented a larger proportion of double-labeled cells than CD3/SIV in LSI-Severe animals (Figure 1-5B).

Correlations between staining for caspase-3, CD3, and CD68 in ileum and colon and intestinal SIV or plasma viral load

In all LSI animals the % ROI positive for CD3 but not CD68 was strongly correlated with SIV infection. After Bonferroni correction, the % ROI positive for CD3 was negatively correlated with the number of cells positive for SIV in the ileum ($r = -0.8330$, $p = 0.0154$) and showed a weak negative correlation in the colon ($r = -0.6900$, $p = 0.1249$) (Figure 1-6A, B). There also was a negative correlation in all LSI animals between the % ROI positive for CD3 and pVL, both in the ileum ($r = -0.9430$, $p = 0.0177$) and colon ($r = -0.8860$, $p = 0.0428$) (Figure 1-6C, D). There were weak negative correlations between the % ROI positive for CD3 and the % ROI positive for caspase-3 in ileum ($r = -0.619$, $p = 0.2300$) and colon ($r = -0.690$, $p = 0.1062$) (Figure 1-6E, F).

In the ileum, the % ROI positive for caspase-3 was positively correlated with pVL ($r = 0.786$, $p = 0.0335$). In the colon, the % ROI positive for caspase-3 was positively correlated with the number of cells positive for SIV ($r = 0.886$, $p = 0.0461$) (Figure 1-6G, H). Further, in all LSI animals regardless of intestinal disease severity, the number of cells positive for SIV RNA was positively correlated with pVL in the ileum ($r = 0.9430$, $p = 0.0188$) and trended positively in the colon ($r = 0.8290$ $p = 0.0875$) (Figure 1-6I).

Direct and indirect measures of microbial translocation in late stage infection

Changes in soluble CD163 (sCD163), which measures increased macrophage activation that might be partially due to increased microbial translocation, were measured via ELISA. The mean rank of sCD163 was significantly different between PC, cART, and LSI animals ($H = 13.09$, $p = 0.0014$). This difference indicated a strong trend towards elevation in sCD163 mean rank in LSI animals with or without intestinal disease vs PC animals ($p = 0.0527$) (Figure 1-7A).

Elevations in plasma soluble CD14 (sCD14) and LPS binding protein (LBP) are thought to result from translocation of microbes and their products, specifically LPS. Plasma sCD14 and LBP were evaluated using ELISA. The mean rank of sCD14 was significantly different between PC, cART, and LSI animals ($H = 6.691$, $p = 0.0352$). These differences indicated significant elevation of sCD14 in cART animals ($p = 0.0388$) and a trend towards elevation in LSI animals with or without intestinal disease ($p = 0.0540$) (Figure 1-7B). LBP mean rank trended similarly to sCD14 between PC, cART, and LSI animals ($H = 4.940$, $p = 0.0846$). This was due to a weak increase in LBP in LSI animals with or without intestinal disease ($p = 0.1531$) (Figure 1-7C) but no change in LBP levels in cART animals.

PCR for microbial 16s rDNA was conducted on plasma, liver, and mesenteric lymph node (MLN) tissue in order to directly detect microbial

translocation. In the plasma a significant difference was found between PC, cART, and LSI animals (H = 10.56, p = 0.0051). This was due to a significant increase in cART animals (p = 0.0024) but not LSI animals (Figure 1-7D). For both the liver and MLN, the median levels of 16s rDNA were not significantly different between PC, cART, and LSI animals (Figure 1-7E, F).

No indicator of microbial translocation correlated with either pVL or terminal CD4 count via Spearman correlation. Further, no group differences were found when LSI animals were subdivided into those with (red squares) or without (black squares) severe intestinal disease.

Of note, for all of the assays except sCD14 several samples primarily in the PC and cART groups tested below the limits of detection for the given assay. As we are using a non-parametric approach to these analyses, which rely on rank-based comparisons, a meaningful statistical conclusion could not be drawn for several comparisons and the data should be therefore considered qualitatively.

CD3 T cell and epithelial claudin-3 loss in the ileum and colon during acute and asymptomatic infection

Ileum and colon of PC, acute (7 days p.i.), and asymptomatic (21 days p.i.) animals were labeled for CD3 and claudin-3 using IHC. There was a significant difference in the mean rank of the % ROI positive for CD3 between PC, acute, and asymptomatic animals in the ileum (H = 8.115, p = 0.0031) and

colon (H = 7.385, p = 0.0145) (Figure 1-8A, B). These group differences represented a significant decrease between the mean rank of the % ROI positive for CD3 between acute and asymptomatic animals in the ileum (p = 0.0134). While only approaching significance, CD3 % ROI trended towards being significantly lower between acute and asymptomatic or PC animals in the colon (p = 0.0558, p = 0.0558). There was no significant difference in the mean rank of % epithelium lacking claudin-3 staining between PC, acute, and asymptomatic animals (Figure 1-8C, D).

Evaluation of epithelial claudin-3 loss and TIA-1 expression in the ileum and colon in late stage infection

Ileum and colon of PC, LSI-None, and LSI-Severe animals were labeled for claudin-3 and TIA-1 using IHC. There was a significant difference in the mean rank of % epithelium lacking claudin-3 staining between PC, LSI-None, and LSI-Severe animals in the ileum (H = 5.808, p = 0.0442) and colon (H = 5.808, p = 0.0442) (Figure 1-8E, F). These group differences represented a significant increase in the mean rank of % loss of claudin-3 between PC and LSI-Severe animals in the ileum (p = 0.0482) and colon (p = 0.0482).

There also was a significant difference in the mean rank of number of TIA-1 positive cells per field between PC, LSI-None, and LSI-Severe animals in the ileum (H = 7.681, p = 0.0071) and colon (H = 8.578, p = 0.0017) (Figure 1-8G, H). These group differences represented a significant increase in the mean rank

of TIA-1 positive cells per field between PC and LSI-None animals in the ileum ($p = 0.0119$) and colon ($p = 0.0075$).

Discussion

The most remarkable findings of this study are that while discrete and severe intestinal disease develops in many late stage SIV-infected animals, those animals that do not develop intestinal disease have intact mucosal T cell populations similar to those in procedural control animals, despite significant declines in T cells in peripheral blood. Further, these T cell populations seem to be a key factor contributing not only to intestinal viral burden but to levels in the plasma as well. These phenomena appear to be independent of macrophage lineage cell populations in the gut despite a large proportion of virus-infected macrophages. Finally, and perhaps most unexpectedly, the presence or severity of enteropathy apparently had little to no impact on levels of microbial translocation in the animals with SIV infection status better predicting translocation.

To our knowledge, this is one of few studies to comprehensively examine the entire gastrointestinal (GI) tract for the cellular and virological effects of SIV in pigtailed macaques. Further, it is the first to describe the effects of SIV on the GI tract in a rapidly progressing macaque model of HIV infection. Of the many microscopic criteria used to evaluate intestinal disease, abnormalities in villous or glandular structure were the most sensitive indicators of enteropathy. Human pathologists have cited similar criteria in HIV-infected patients as reliable indicators of intestinal disease (3, 4). Anatomically, the ileum and colon were the sites that exhibited the most severe pathological changes. This suggests that examination of villus and glandular structure in the ileum and colon are the most

efficient method for evaluating SIV-induced enteropathy in pigtailed macaques and likely other non-human primates.

Some histopathological features in the gut of rapidly progressing SIV-infected pigtailed macaques reflect previous observations in SIV/HIV-infected macaques and humans, while others appear unique to this model. In particular, histopathological evidence of enteropathy did not arise until 56 days post inoculation, when the macaques are undergoing the early stages of systemic immune depletion and recrudescence of plasma and tissue viral loads. Statistically significant pathological changes in the gut were not present until late stage disease, approximately three months post inoculation. This is in contrast to humans and the SIV/rhesus macaque model in which enteropathy appears early in infection and the histological lesions are sustained (3, 12, 24).

We examined three groups of late stage SIV-infected animals: those with mild (LSI-Mild), severe (LSI-Severe), or no (LSI-None) intestinal disease. There was a highly significant positive correlation between intestinal disease severity scores and plasma viral load for all LSI animals with intestinal disease (LSI-Mild & LSI-Severe), and a strong negative correlation between terminal blood CD4+ T cell counts and severity of intestinal disease in LSI-Severe animals. This indicates that the GI tract is either sensitive to, or responsible for dramatic changes in systemic viral replication and associated systemic immunological dysfunction during chronic infection.

Intestinal disease in animals treated with combination antiretroviral therapy (cART) was absent, similar to procedural control (PC) animals suggesting that cART initiated during acute infection was effective at preventing the development of intestinal disease. This was also true in all gut sites examined. Numerous studies have examined the effectiveness of cART in restoring dysfunction of the gut in HIV-infected people. This has most thoroughly been evaluated by measuring restoration of CD4+ T cell populations in the gut with mixed results. Early intervention, similar to the cART regimen we used, often results in restoration of CD4+ T cells in various intestinal regions; later intervention is typically insufficient. (25)

To better understand alterations to cellular processes and populations in the GI tract, we quantified cells undergoing apoptosis, the numbers of CD3+ T cells and CD68+ macrophages, and the relative numbers of SIV infected T cells and macrophages in PC, LSI-Severe and LSI-None animals. Increased caspase-3 expression and TUNEL labeling as well as reduced tight junction proteins have been detected in chronically HIV-infected humans and SIV-infected macaques. These are associated with a dysfunctional gut barrier (12, 28, 29). In this study, LSI-Severe animals had a significant increase in caspase-3 immunohistochemical staining in the ileum and trended towards an increase in the colon. These increases coincided with a shift in the location of positively stained cells from the superficial mucosa on villus tips and between colonic glands in PC and LSI-None animals, to discrete foci concentrated around degenerating villi and glands in LSI-Severe animals. These findings provide

experimental support for our histological observations that villus/glandular disruption might be the most predictive histological finding of intestinal disease.

It is widely known that the gut is a site of rapid HIV/SIV replication and loss of CD4+ T cells during acute infection, and that the GI tract does not typically recover from this damage (5, 6). In this study, there was no change to the organization of T cells in the gut between PC and LSI animals; CD3+ staining was evenly distributed throughout the lamina propria. However, in both the ileum and colon there was a significant and dramatic reduction in the amount of CD3 staining in LSI-Severe animals. These findings agree with observations that T cell populations are ablated and do not recover after acute infection. However, concentrations of T cells in LSI-None animals were similar to those in uninfected animals demonstrating a previously unreported preservation of T cell populations in some chronically infected late stage animals.

Some studies in untreated HIV-infected individuals have reported increased numbers of macrophages in the gut, perhaps due to their relative resistance to lytic HIV infection, and alterations in macrophage phenotype away from an inflammatorily anergic state towards a pro-inflammatory state in the gut (26-29, 8, 9). In this study, CD68+ cells in PC animals were found primarily in the peri-luminal portions of the villi in the ileum and glands in the colon. However, in LSI-Severe animals large numbers of CD68+ macrophages were detected surrounding foci of villus and glandular degeneration. In the colon there was a significant reduction in the level of CD68 immunostaining in LSI-Severe compared to PC animals. The decrease was found only in the colon, which

suggests that different environmental conditions exist in the colon and ileum that result in loss of macrophages in the colon only. These results are distinguished from the typical finding of preservation and even expansion of macrophage populations in the gut during SIV and HIV infection.

The gut is a site of intense viral replication in acutely infected humans and macaques and of ongoing viral replication in the absence of cART. LSI-Severe animals had a significant increase in the number of virus-infected cells in the ileum and a trend towards an increase in the colon as compared to LSI-None animals. This increased viral replication was occurring despite tremendous depletion of T cells in both sites in LSI-Severe animals. There was an increase in the proportion of SIV-infected macrophages in LSI-Severe animals as compared to LSI-None. Again, this is despite reduction in the numbers of macrophages in the colon of LSI-Severe animals. These findings are unique as we saw low numbers of virus-infected cells in some LSI-None animals despite preservation of T cell populations and high viral loads in the plasma.

There was a highly significant negative correlation between the number of SIV-positive cells and the level of CD3 staining, but not CD68 staining in the ileum of all LSI animals. A similar strong correlation trended towards significance in the colon. There also was a strong negative correlation between plasma viral load and level of CD3 staining, but not CD68 staining, in the ileum and colon. CD3 also showed a weak, negative correlation with caspase-3 staining. There was a strong positive correlation between caspase-3 staining and the number of SIV-infected cells in the ileum, and plasma viral load in the colon. Finally, the

number of cells positive for SIV in the ileum and colon positively correlated with the amount of virus in the plasma. It should be noted that despite having only 8 samples per comparison these correlations were very strong.

These data taken together with the histological observations indicate that intestinal disease in this model coincides with increased viral replication, both in the gut and blood, and the subsequent loss of T cells. Nonetheless, only about 50% of animals with high viral loads and loss of peripheral blood T cells develop intestinal disease. Further, these data suggest that T cells and not macrophages are the primary contributors or regulators of virus production in the gut. This T cell-derived viral pool in the gut has a very strong relationship with the level of virus in the plasma regardless of the density of intestinal T cells and level of intestinal disease in the animal. This would indicate that in this model the gut is more reflective of the blood as a viral compartment and not the spleen or brain, which are primary influenced by macrophage infection and inflammation (30, 31).

Indeed, GI tract macrophages arise from a lineage independent of many other tissue sites. They are primarily derived from blood monocytes and not the embryonically seeded progenitors that populate the spleen and brain (32). Perhaps late stage SIV infection in this model captures a physiological state close to death where loss of GI tract macrophages in the large intestine might be due to destruction of the seeding pool of blood monocytes and not reflective of direct infection of GI tract macrophages (33).

Unique to this study is the finding that gut T cell populations are preserved in late stage infection in the absence of enteropathy in a large proportion of animals. Plasma viral load and terminal CD4+ T cell counts only correlated with those LSI animals exhibiting intestinal disease whereas the level of CD3 staining in the gut correlated with plasma viral load for all LSI animals indicating that intestinal disease is secondary to the health of the gut T cell population. This agrees with the concept that lack of recovery of CD4 populations in the gut with cART therapy in humans predicts a poor clinical outcome.

Microbial translocation is a thought to be a common occurrence in chronically HIV-infected individuals and in those on cART, resulting from early destruction of the T cell populations in the gut and associated epithelial disruption (14-17). However, especially in people on cART, the relationship between T cells, intestinal damage, translocation, and inflammation is not clear. We examined several markers of microbial translocation in all groups of animals. Regardless of the assay used, there was no difference between LSI-None and LSI-Severe animals. All LSI animals had significantly increased plasma sCD163, a marker of macrophage activation, and plasma sCD14, a marker of macrophage and monocyte response to LPS as compared to procedural controls. In addition, plasma sCD14 was elevated in cART animals despite the absence of any intestinal damage. Plasma LBP was somewhat elevated in LSI animals, although this finding was not statistically significant.

We also examined levels of 16s rDNA in plasma, MLN, and liver. Plasma levels of 16s rDNA were increased in cART animals. The majority of LSI animals

had more plasma 16s rDNA than PC animals but not significantly so. There were no significant increases observed in the MLN or liver. The sensitivity of 16s rDNA qPCR might be inferior to that of other assays given the nature of endogenous DNAse activity by the host and 16s rDNA has been shown to be a poorer predictor of translocation and clinical outcome when compared to other assays (34).

The observation that there were little to no differences in measures of microbial translocation between LSI-None and LSI-Severe animals was unexpected. Most studies indicate that increased intestinal disease and loss of T cell populations in the gut coincide with increased microbial translocation. Additionally, in some human studies and some NHP models this has been reported to occur acutely and set the stage for ongoing inflammation throughout the course of disease. Our data suggest that while microbial translocation is indeed increased during late stage infection, it appears to be independent of the severity of intestinal disease. Interestingly, no measurement of microbial translocation correlated with CD3 or CD68 staining, or the number of virus-infected cells in the gut. While these findings are surprising when compared with untreated chronic HIV or other models of SIV infection, they agree with some of the findings in treated humans where acute cART might preserve T cell populations and result in reduced bacterial burden and a positive clinical outcome (35, 36).

To further elucidate a reason for the apparent lack of microbial translocation in this model we examined animals euthanized at 7 and 21 days

post infection (acute and asymptomatic) despite their lack of intestinal disease. In agreement with majority of the literature on the topic we saw significantly lower numbers of CD3 positive T cells in animals 7 days after infection. However, this apparent loss of T cells during acute infection did not coincide with any increased indicators of intestinal disease via histopathological examination. Further, T cell populations at 21 days post infection had recovered to levels similar to those seen in uninfected animals in the ileum and colon. The recovery of T cell populations after acute infection, in the absence of cART in this model differs with conventional thinking on this topic.

Looking beyond overt histological indications of intestinal disease we sought to evaluate intestinal epithelium integrity directly via the tight junction associated protein claudin-3. Tight junction complexes are one of several mechanisms that prevent the translocation of microbes across the intestinal mucosa. These complexes respond to inflammation in the gut mucosa (37) and are directly affected by HIV at least in vitro (38). In spite of a significant losses of T cells 7 days post infection we did not see an accompanying loss of epithelial claudin-3 during acute or asymptomatic infection; findings that support the lack of intestinal disease observed via histological evaluation.

We also evaluated the integrity of the epithelial barrier during late stage infection where some epithelial degradation was observed in some animals on histological evaluation. Interestingly, animals that exhibited severe intestinal disease had a significant increase in the % loss of claudin-3 staining in the

epithelium compared to PC animals. This loss was not observed in animals lacking intestinal disease.

Theorizing about potential drivers of intestinal disease in this model, we sought to quantitate the number of cytotoxic T lymphocytes (CTLs) in the intestinal mucosa. CTLs have the potential to increase epithelial apoptosis through a maladaptive inflammatory response to HIV or other intracellular pathogens and have been implicated in contributing at least in part to epithelial damage during acute HIV infection (39). Opposite of our expectations, the number of cells containing TIA-1, a protein associated with the pro-apoptotic cytoplasmic granules in CTLs, was elevated in LSI-None animals, not LSI-Severe animals. While on the surface counterintuitive, this might suggest that preservation of CTL populations confers a type of intestinal resilience absent in animals who develop intestinal disease. An increase in PD-1 expression on SIV-specific CTLs in the intestines during chronic infection which coincides with functional impairment of adaptive CTL responses has been reported in SIV infected rhesus macaques that develop intestinal dysfunction and exhibit microbial translocation throughout disease (40). Thus, it is possible that in these animals a more robust SIV specific CTL response might, in part, be responsible for attenuating both intestinal disease and microbial translocation; and when these cells are lost, intestinal dysfunction occurs.

A number of potential mechanisms could drive intestinal damage other than CD4+ T cell destruction with functional impairment and loss of virus-specific CTLs. Dendritic cells, both plasmacytoid (pDCs) and myeloid, are CD68 negative

and can be infected by HIV. Proliferative pDCs have been reported to infiltrate the gut of HIV-infected individuals and up regulate the pro-apoptotic enzyme granzyme B (41). Additionally, pro-inflammatory mucosal mDCs can be productively infected and are linked to microbial population changes (42). These features of inflammation and proliferation in DCs might allow them to contribute to observed enteropathy.

Shifts in the microbiota of the gut have been reported both in chronically infected and cART treated humans and macaques and are associated with disease progression. Specific taxa are associated with favorable or unfavorable conditions in treated HIV patients. Two examples are increased Proteobacteria and proinflammatory tryptophan metabolism (43), and increased Lactobacillales and reduced microbial translocation (44). Perhaps the predominant type of bacteria that are present and translocating is influencing the gut in unforeseen ways.

Given the rapid progression of disease in this model, it's possible that highly pro-inflammatory microbial translocation only arises with prolonged intestinal barrier impairment and not acute episodes of increased inflammation. Indeed our experiments indicate that, at least in this model, the first bouts of microbial translocation are likely to occur during late stage infection and not in acute infection. This is unique in the body of literature regarding microbial translocation during HIV and SIV infection. This model has been previously shown to recapitulate many aspects of HIV associated inflammation and immunological impairment making these findings regarding translocation all the

more important. Indeed there are likely other mechanisms involved such as viral escape from host control, and further study is warranted.

Our findings highlight the complexities around chronic inflammation in HIV or SIV disease. Collectively these findings support the need for continued study of the nature of enteropathy in HIV-infected patients through clinical monitoring as well as SIV/macaque modeling. Additionally, we feel there is a discrete need for more rigorous approaches and assays to evaluate the presence and amount of microbial translocation occurring in the host. Ideally, these data along with those from other NHP models of HIV will provide new avenues of therapy and allow further improvement of the lives of those affected.

Acknowledgements

Anti-retroviral drugs for macaques used in this study were generously donated by Gilead (tenofovir), Bristol-Myers Squibb (atazanavir), Merck (integrase inhibitor L000870812 / INSTI), Hoffmann La Roche (saquinavir). Additionally, special thanks are given to the excellent veterinary care staff at Johns Hopkins University School of Medicine.

Group Name	Abbreviation	N	Infected	Days PI	Treatment
Procedural Control	PC	12	No	84-90	
Day 4	4d	8		4	
Day 7	7d	6		7	
Day 10	10d	6		10	
Day 14	14d	6		14	No
Day 21	21d	6	Yes	21	
Day 42	42d	9		42	
Day 56	56d	9		56	
Late Stage Infected	LSI	25		60-101 (Terminal)	
cART	cART	5		161-175	cART

Table 1-1. Animal euthanasia dates and treatments.

	PC			cART			LSI		
	Mean	**Median**	**Pos**	**Mean**	**Median**	**Pos**	**Mean**	**Median**	**Pos**
Giant Cells	0	0	0	0	0	0	4.08	2	58.3
Mixed Infiltrates	8.58	8.5	100	10.4	11	100	10	10	100
Epithelium Integrity	0.83	0	16.7	0.4	0	20	1.29	0	45.8
Villus/Gland Abnormality	0.08	0	8.3	0	0	0	2.83	2	66.7

Table 1-2. Intestinal disease scoring descriptive statistics.

Figure 1-1

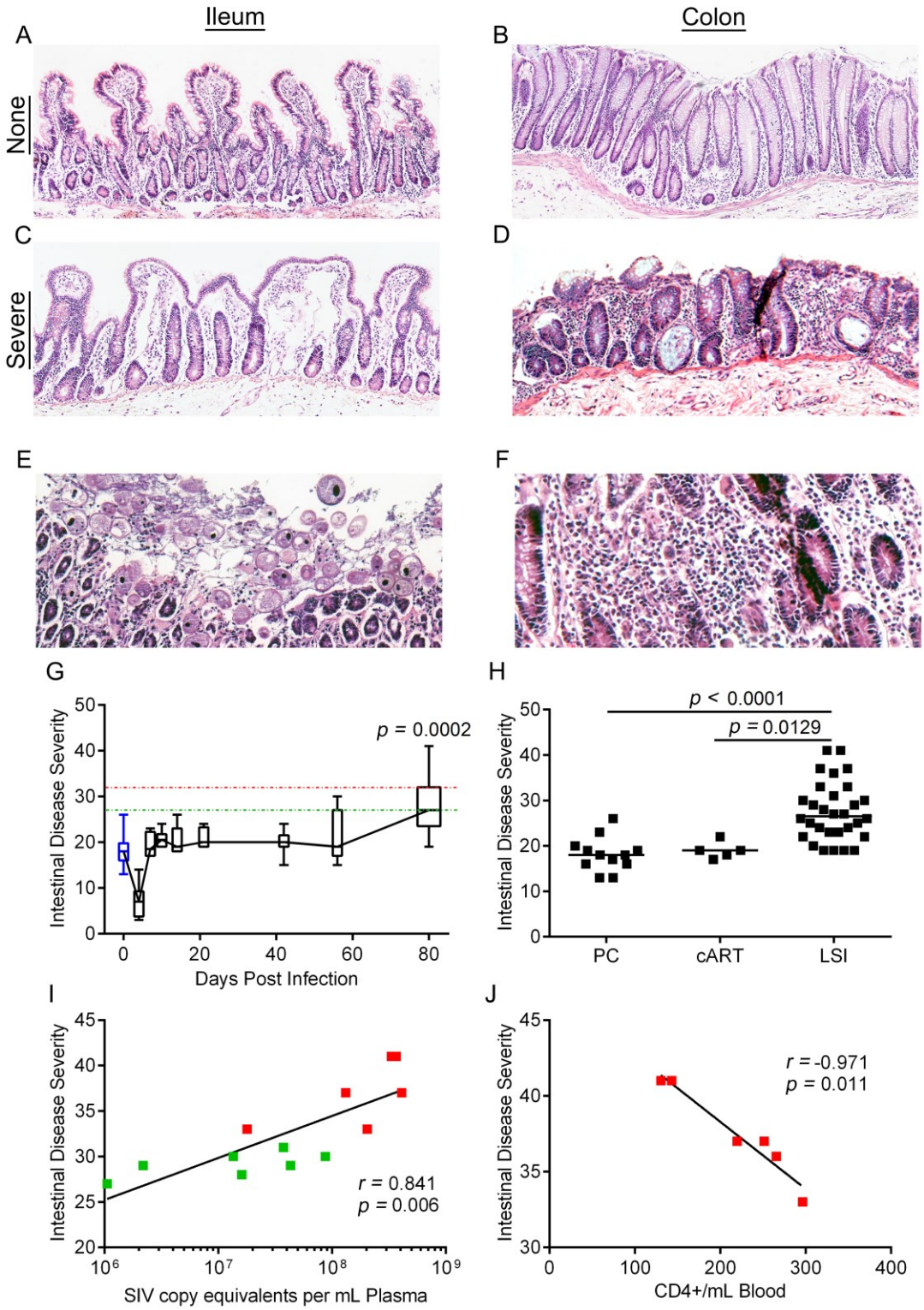
Ileum
Colon
A
B
None
C
D
Severe
E
F
G
H
p = 0.0002
Intestinal Disease Severity
Days Post Infection
p < 0.0001
p = 0.0129
PC
cART
LSI
I
J
r = 0.841
p = 0.006
SIV copy equivalents per mL Plasma
r = -0.971
p = 0.011
CD4+/mL Blood

Figure 1-1. Intestinal disease scores in uninfected, SIV-infected cART treated, and SIV-infected untreated pigtailed macaques. Intestinal disease was evaluated in procedural control (PC), SIV-infected animals euthanized at days 4, 7, 10, 14, 21, 42, 56 post infection, late stage SIV-infected (LSI) animals, and SIV-infected animals on combination antiretroviral therapy (cART). **A, B)** H&E tissue sections of ileum (left) and colon (right) from a LSI animal with no intestinal disease. **C, D)** H&E tissue sections of ileum (left) and colon (right) from a LSI animal with severe intestinal disease. **E)** Representative *Balantidium coli* overgrowth and associated tissue damage in colon of a LSI severe animal. **F)** Representative multinucleated giants cells in the colon of a LSI severe animal. **G)** PC (Blue) and longitudinal intestinal disease scores. **H)** Comparison of intestinal disease scores between PC, cART, and LSI animals. **I)** Spearman correlation between intestinal disease score and plasma viral load (pVL) **J)** Spearman correlation between intestinal disease score and terminal CD4+ T cell count. Green and red squares indicate LSI animals with mild or severe intestinal disease respectively. Exact *p* values between groups were calculated by Kruskal-Wallis test followed by Dunn's post hoc correction.

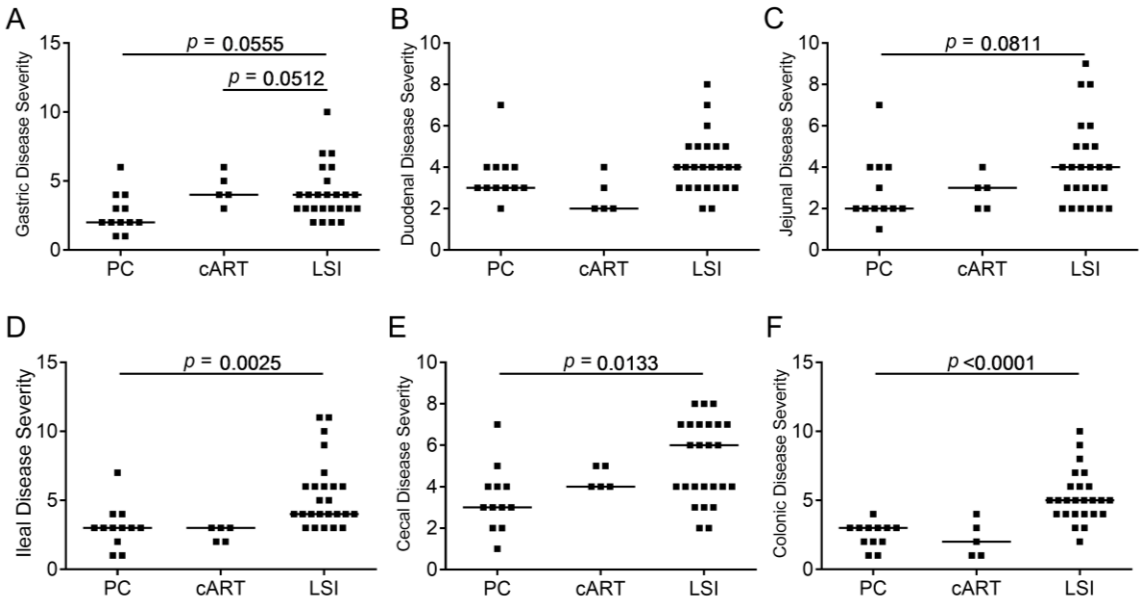

Figure 1-2. Intestinal disease by tissue site in uninfected, SIV-infected cART treated, and SIV-infected, untreated pigtailed macaques. Intestinal disease in six intestinal sites were evaluated in procedural control (PC), terminally SIV-infected (TI) animals, and SIV-infected animals on combination antiretroviral therapy (cART). **A)** Stomach **B)** Duodenum **C)** Jejunum **D)** Ileum **E)** Cecum **F)** Colon. Exact *p* values between groups were calculated by Kruskal-Wallis test followed by Dunn's post hoc correction.

Figure 1-3

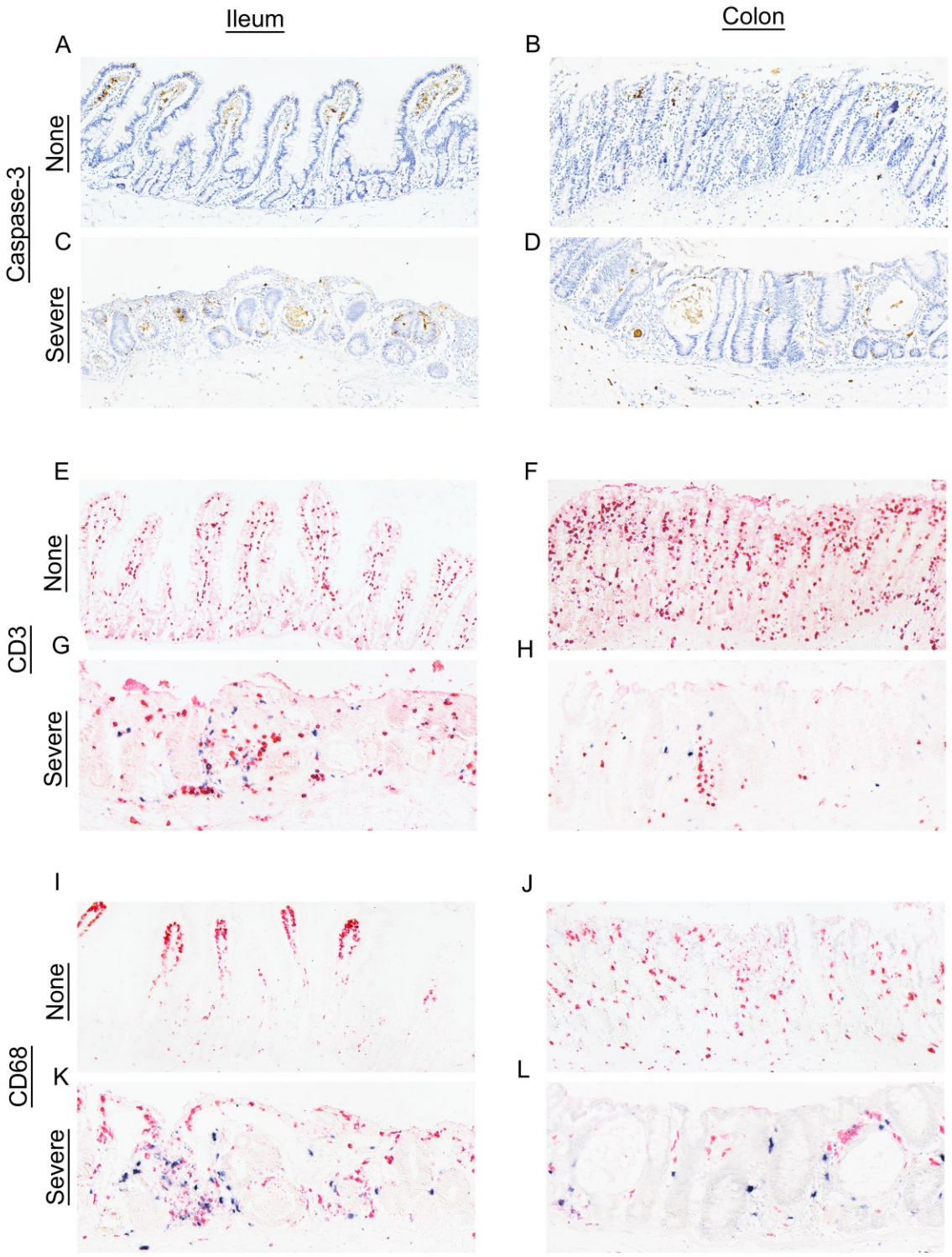
Ileum
Colon
A
B
C
D
Caspase-3
None
Severe
E
F
G
H
CD3
None
Severe
I
J
K
L
CD68
None
Severe

Figure 1-3. Representative images of caspase-3, CD3, CD68, and SIV expression. IHC and ISH in the ileum (left column) and colon (right column) of late stage infected (LSI) animals. **A, B)** Caspase-3 staining of LSI animals without intestinal disease. **C, D)** Caspase-3 staining of LSI animals with severe intestinal disease. **E, F)** CD3 & SIV staining of LSI animals without intestinal disease. **G, H)** CD3 & SIV staining of LSI animals with intestinal disease. **I, J)** CD68 & SIV staining of LSI animals without intestinal disease. **K, L)** CD68 & SIV staining of LSI animals with intestinal disease. All images were taken at 100x magnification.

Figure 1-4

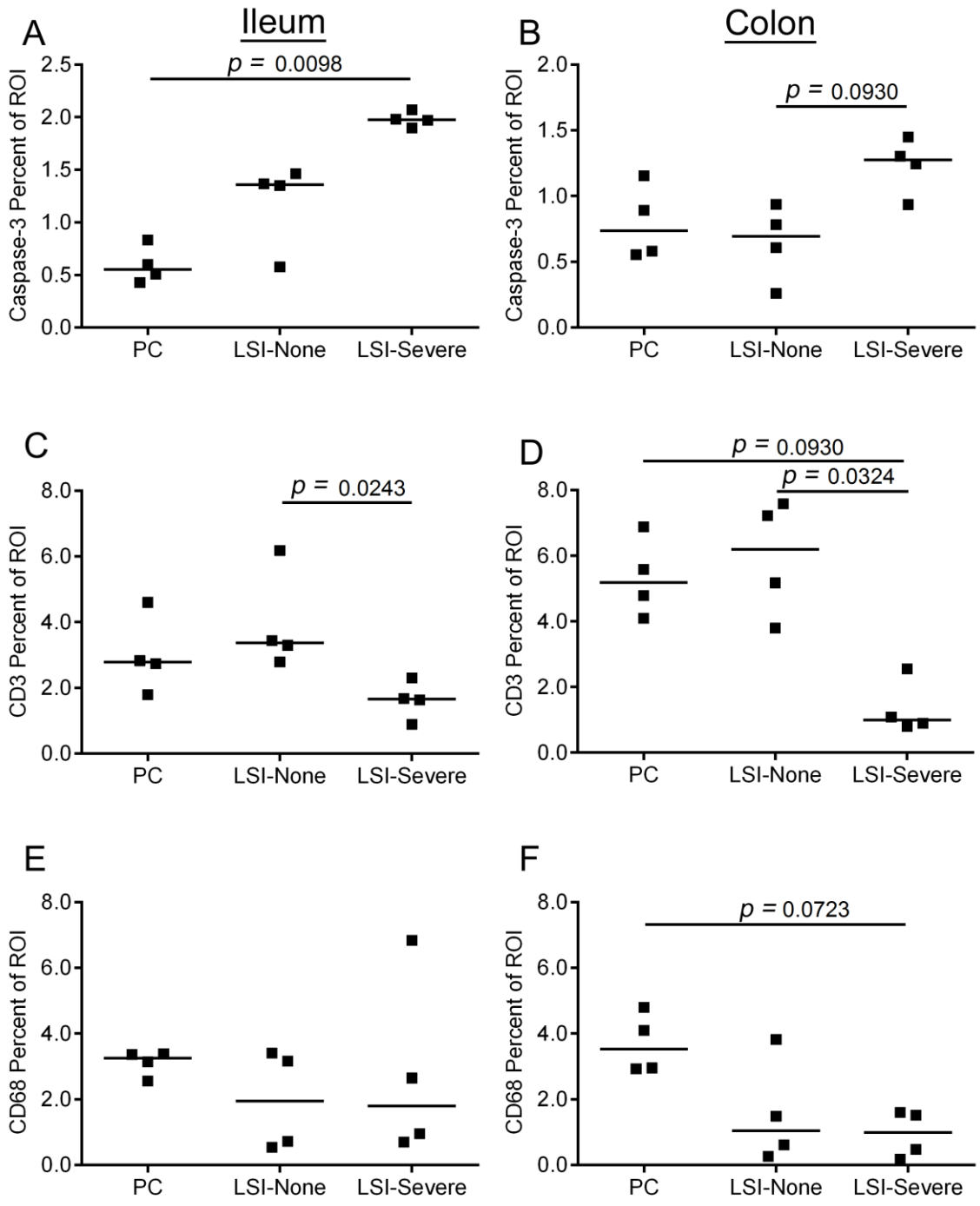
A
Ileum
p = 0.0098
Caspase-3 Percent of ROI
2.5
2.0
1.5
1.0
0.5
0.0
PC
LSI-None
LSI-Severe
B
Colon
p = 0.0930
Caspase-3 Percent of ROI
2.0
1.5
1.0
0.5
0.0
PC
LSI-None
LSI-Severe
C
p = 0.0243
CD3 Percent of ROI
8.0
6.0
4.0
2.0
0.0
PC
LSI-None
LSI-Severe
D
p = 0.0930
p = 0.0324
CD3 Percent of ROI
8.0
6.0
4.0
2.0
0.0
PC
LSI-None
LSI-Severe
E
CD68 Percent of ROI
8.0
6.0
4.0
2.0
0.0
PC
LSI-None
LSI-Severe
F
p = 0.0723
CD68 Percent of ROI
8.0
6.0
4.0
2.0
0.0
PC
LSI-None
LSI-Severe

Figure 1-4. Quantitation of caspase-3, CD3, and CD68 immunohistochemistry (IHC). Percent region of interest (%ROI) positive by IHC in the ileum (left column) and colon (right column) of procedural control (PC) and late stage SIV-infected (LSI) animals with and without severe intestinal disease. **A, B)** Caspase-3 staining in PC, and LSI animals with or without intestinal disease. **C, D)** CD3 & SIV staining in PC, and LSI animals with or without intestinal disease. **E, F)** CD68 & SIV staining in PC, and LSI animals with or without intestinal disease. Exact *p* values between groups were calculated by Kruskal-Wallis test followed by Dunn's post hoc correction.

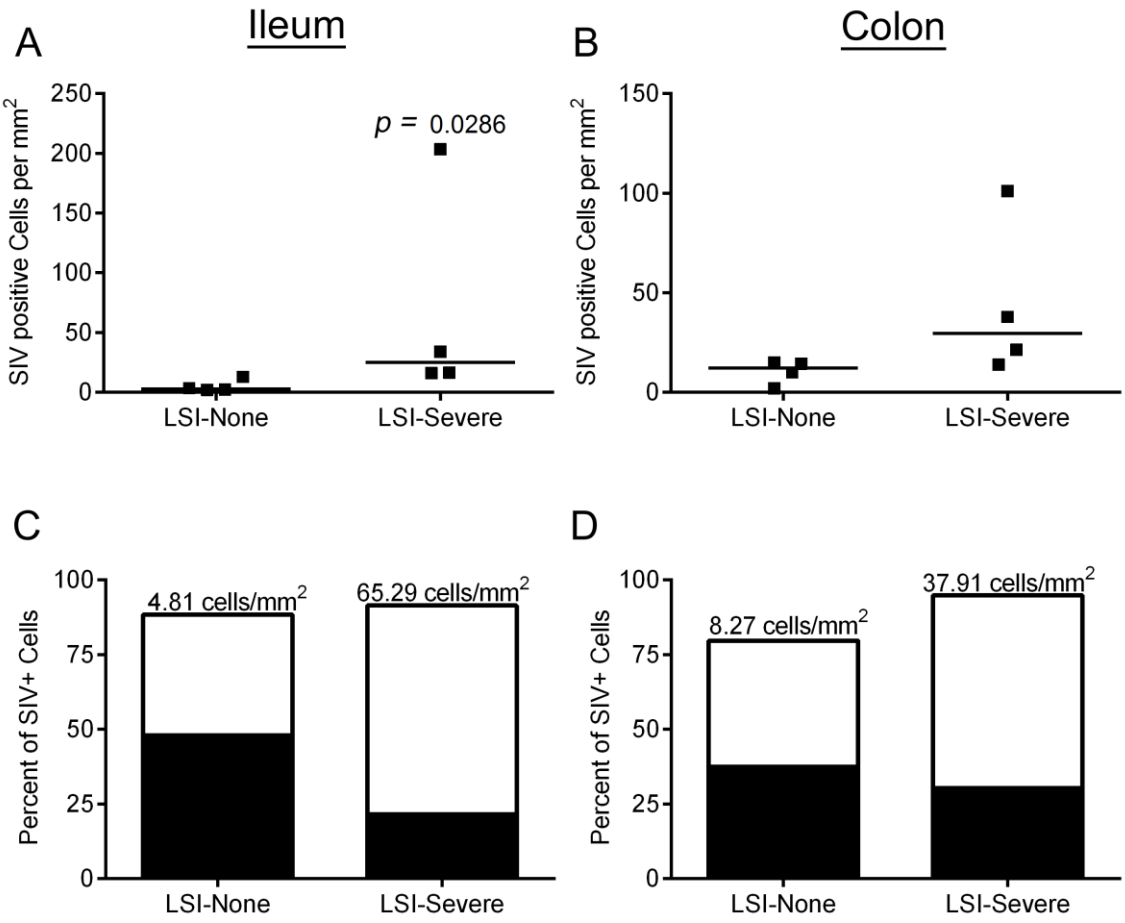

Figure 1-5. Quantitation of SIV by *in situ* hybridization (ISH). The number of cells positive by ISH for SIV in the ileum (left column) and colon (right column) of late stage SIV-infected (LSI) animals with and without severe intestinal disease. **A, B)** Total cells singly positive for SIV. **C, D)** Percent of cells double labeled for SIV and CD3 or SIV and CD68. Numbers on bar graphs are the average total number of cells double-positive for SIV and CD3 or CD68 normalized to one mm^2. Exact *p* values between groups were calculated by Mann-Whitney test.

Figure 1-6

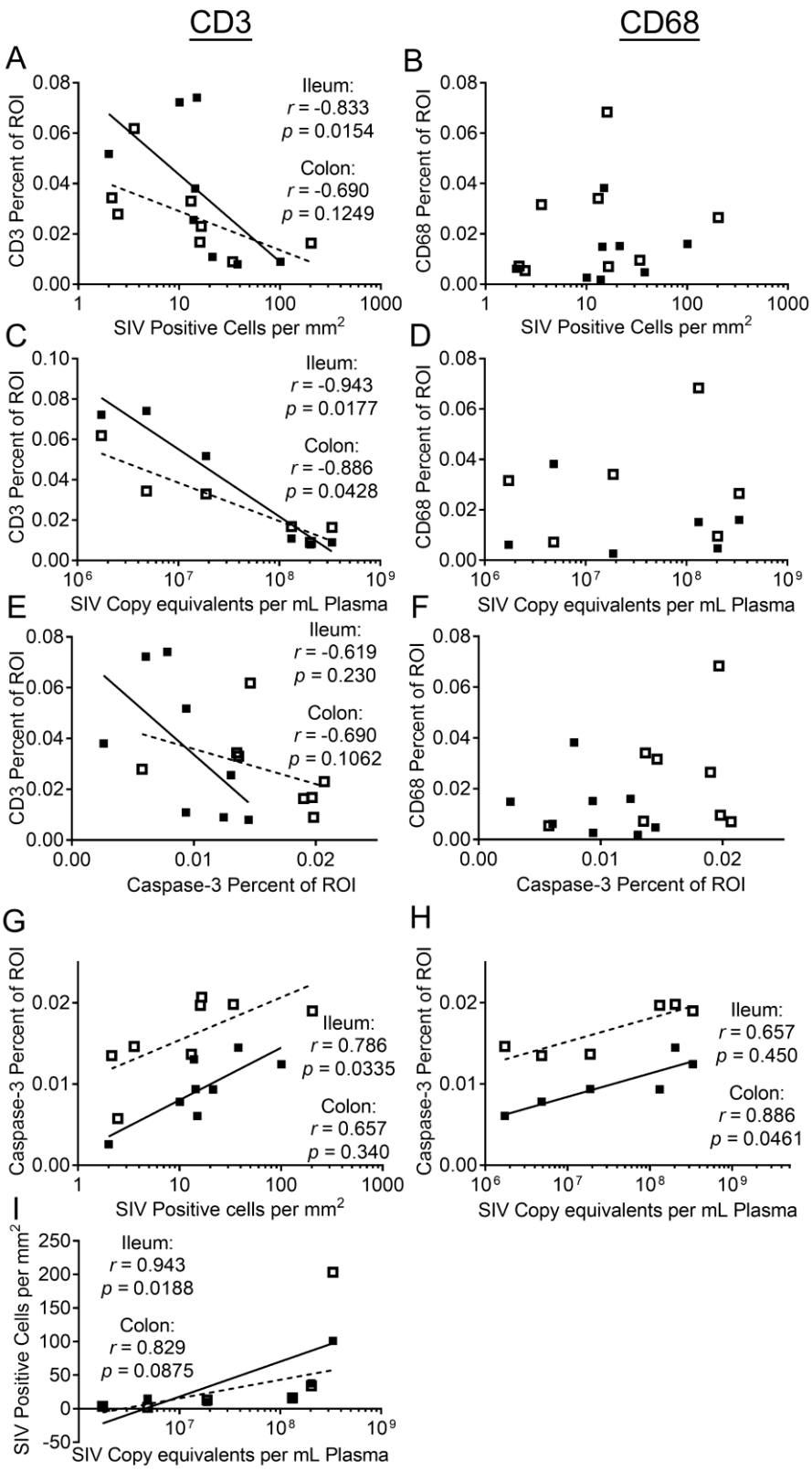
CD3
CD68
A
B
C
D
E
F
G
H
I
CD3 Percent of ROI
CD68 Percent of ROI
SIV Positive Cells per mm2
SIV Copy equivalents per mL Plasma
Caspase-3 Percent of ROI
SIV Positive cells per mm2
Ileum:
r = -0.833
p = 0.0154
Colon:
r = -0.690
p = 0.1249
Ileum:
r = -0.943
p = 0.0177
Colon:
r = -0.886
p = 0.0428
Ileum:
r = -0.619
p = 0.230
Colon:
r = -0.690
p = 0.1062
Ileum:
r = 0.786
p = 0.0335
Colon:
r = 0.657
p = 0.340
Ileum:
r = 0.657
p = 0.450
Colon:
r = 0.886
p = 0.0461
Ileum:
r = 0.943
p = 0.0188
Colon:
r = 0.829
p = 0.0875

Figure 1-6. Relationship between CD3 or CD68 immunohistochemistry (IHC) and SIV in gut or plasma. Relationships between markers of interest for all late stage SIV-infected (with and without severe intestinal disease) animals were examined in the ileum (closed squares) and colon (open circles) **A)** Relationship between CD3 and total number of SIV positive cells. **B)** Relationship between CD68 and total number of SIV positive cells. **C)** Relationship between CD3 and plasma viral load (pVL). **D)** Relationship between CD68 and pVL. **E)** Relationship between CD3 and caspase-3 **F)** Relationship between CD68 and caspase-3 **G)** Relationship between caspase-3 and total number of SIV positive cells. **H)** Relationship between caspase-3 and pVL. **I)** Relationship between total number of SIV positive cells and pVL. Spearman's coefficient and post Bonferroni correction exact *p* values for each analysis are reported where relevant.

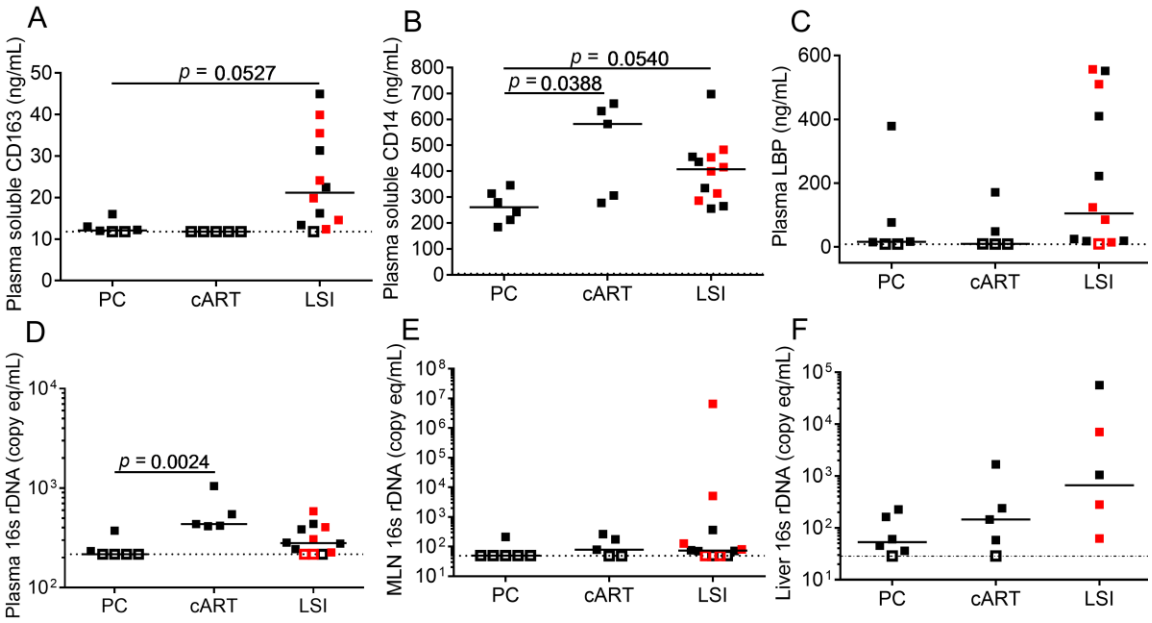

Figure 1-7. Direct and indirect measures of microbial tranlocation and associated inflammation during late stage disease. ELISAs (top row) and quantitative PCRs (bottom row) were conducted on samples from procedural control (PC), terminally SIV-infected (TI) animals with (red squares) and without (black squares) severe intestinal disease, and SIV-infected animals on combination antiretroviral therapy (cART). **A)** Plasma soluble CD163 **B)** Plasma soluble CD14 **C)** Plasma LPS binding protein **D)** Plasma 16s ribosomal DNA **E)** Mesenteric lymph node 16s ribosomal DNA **F)** Liver 16s ribosomal DNA. Open symbols represent samples that were below the given assays limit of detection. Exact *p* values between groups were calculated by Kruskal-Wallis test followed by Dunn's post hoc correction.

Figure 1-8

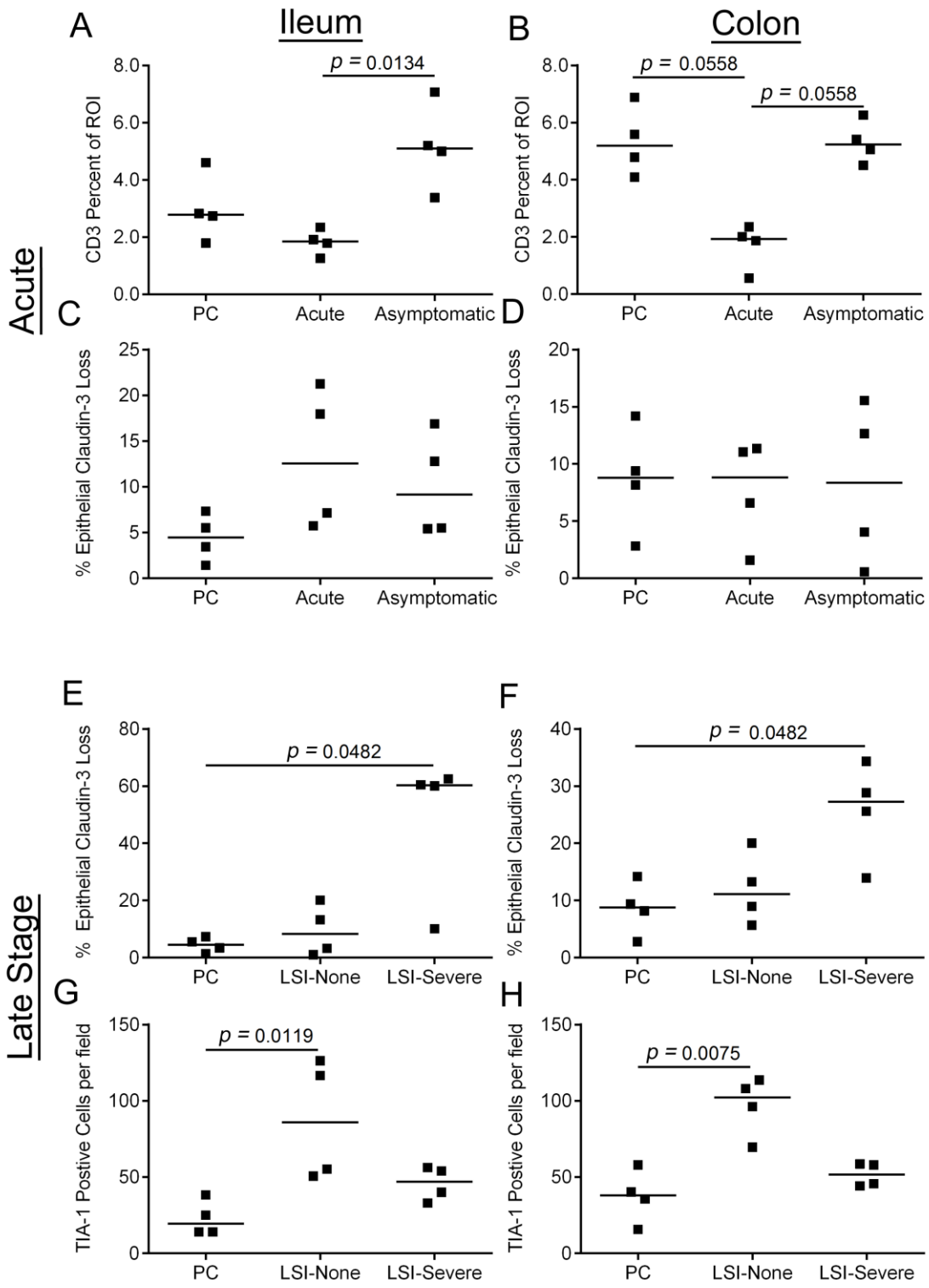
A
Ileum
B
Colon
Acute
p = 0.0134
p = 0.0558
p = 0.0558
CD3 Percent of ROI
8.0
6.0
4.0
2.0
0.0
PC
Acute
Asymptomatic
C
D
% Epithelial Claudin-3 Loss
25
20
15
10
5
0
E
F
Late Stage
p = 0.0482
p = 0.0482
80
60
40
20
LSI-None
LSI-Severe
G
H
TIA-1 Postive Cells per field
p = 0.0119
p = 0.0075
150
100
50

Figure 1-8. Quantitation of CD3, claudin-3 and TIA-1 immunohistochemistry (IHC). Percent region of interest (%ROI) positive for CD3 and percent epithelial claudin-3 loss (%Loss) by IHC during acute and asymptomatic infection (top two rows). Average number of TIA-1 positive cells per field and percent epithelial claudin-3 loss (%Loss) by IHC in late stage SIV-infected (LSI) animals with and without severe intestinal disease in the ileum (left column) and colon (right column). **A, B)** CD3 staining in PC, day 7 post infection (acute), and day 21 post infection (asymptomatic). **C, D)** Claudin-3 staining in PC, day 7 post infection (acute), and day 21 post infection (asymptomatic). **E, F)** Claudin-3 staining in PC, and LSI animals with or without intestinal disease. **G, H)** TIA-1 staining in PC, and LSI animals with or without intestinal disease. Exact *p* values between groups were calculated by Kruskal-Wallis test followed by Dunn's post hoc correction.

All Animals

	Stomach	Duod.	Jejunum	Ileum	Colon	Cecum
Giant Cells	14	34	38	36	46	55
Mixed Infiltrates	132	177	155	136	137	150
Epithelium Integrity	8	4	6	25	14	27
Villus/Gland Abnormality	7	15	23	45	26	9

Supplemental Table 1-1. Sum of scores for each indicator of intestinal disease in late stage infected animals.

Giant Cells

	Stomach	Duodenum	Jejunum	Ileum	Colon	Cecum
PC	-	-	-	-	-	-
cART	-	-	-	-	-	-
LSI	0.13	0.4	0.67	0.73	1	1.23

Infiltrates

	Stomach	Duodenum	Jejunum	Ileum	Colon	Cecum
PC	0.92	2.00	1.42	1.42	1.33	1.50
cART	2.20	1.60	1.60	1.40	1.60	2.00
LSI	1.52	1.92	1.75	1.58	1.58	1.63

Epithelium Integrity

	Stomach	Duodenum	Jejunum	Ileum	Colon	Cecum
PC	-	-	-	-	-	0.17
cART	-	-	-	-	-	0.40
LSI	0.33	0.08	0.08	0.33	0.25	0.21

Villus/Gland Abnormal

	Stomach	Duodenum	Jejunum	Ileum	Colon	Cecum
PC	-	-	0.08	-	-	-
cART	-	-	-	-	-	-
LSI	0.21	0.41	0.54	0.88	0.54	0.25

Supplemental Table 1-2. Average score by intestinal disease indicator and animal group.

Intestinal Disease Category Versus Total Enteropathy

	r	r^2	p
Giant Cells	0.48	0.23	< 0.0001
Mixed Infiltrates	0.26	0.07	0.01
Epithelium Integrity	0.41	0.17	< 0.0001
Villus/Gland Abnormality	0.50	0.25	< 0.0001

Supplemental Table 1-3. Pearson's correlations between each indicator of intestinal disease and overall disease score.

CHAPTER III.

Maraviroc with cART Improves Restoration of Memory T Cell Populations Over cART Alone in the Blood and Organs of SIV Infected, Suppressed, Pigtailed Macaques

This Chapter has been prepared as a manuscript for submission to the *Journal of Infectious Disease* for publication consideration.

Abstract

Combination antiretroviral therapy (cART) fails to correct immunological imbalances acquired during acute Human immunodeficiency virus (HIV) infection. cART-treated HIV-infected patients exhibit alterations to numbers and activation of memory T cells. Using a rapidly progressing SIV/pigtailed macaque model of HIV we examined naive, central, and effector memory T cells, and expression of CD27, CCR5, CCR7, and HLA-DR in the blood, gut, and draining gut and peripheral lymph nodes in uninfected, late stage infected (LSI), animals receiving cART, and cART plus Maraviroc (cART+M) using flow cytometry. The number of $CD4^+$ T cells was lower in the blood and gut of LSI animals and was restored with cART and cART+M in the blood and colon. cART+M animals had improved restoration of $CD4^+$ and $CD8^+$ naive and central memory T cells over cART alone in the gut. cART+M animals had markedly increased CD27 expression on naïve, central, and effector $CD4^+$ memory T cells in all body regions; and on central, and effector $CD8^+$ memory T cells in the ileum and colon indicating earlier differentiation of cells. Finally, reductions were observed to CCR7 in the blood and HLA-DR in the gut on $CD4^+$ and $CD8^+$ memory T cells indicating a reduction in activation of T cells.

Introduction

Human immunodeficiency virus (HIV) infection can be effectively controlled with modern combination antiretroviral therapy (cART). However, cART therapy does not fully reverse some immunological dysfunction acquired during acute disease such as $CD4^+$ T cell loss in the jejunum (1, 2). This $CD4^+$ T cell dysfunction is associated with impairment of the intestinal mucosa's ability to regulate pro-inflammatory responses to the microbiota (3). Impairment of the intestinal immune system is central to theories explaining the chronic immunological imbalance in HIV-infected patients receiving cART. Intestinal inflammation is triggered by active microbial translocation resulting in contamination of the lymphatic fluid and blood with microbial pyrogens. Various markers of microbial translocation, principally lipopolysaccharide (LPS) have been inversely correlated with immunological restoration and used to predict long term clinical improvement (4, 5, 6). Other mechanisms might also provide a path to microbial pyrogen dissemination such as dendric cell (mDC) and macrophage migration (7, 8).

Not only does HIV drive systemic inflammation through destruction of $CD4^+$ T cells but also by altering the immunological memory of both $CD4^+$ and $CD8^+$ T cells. Naïve ($CD28^-$, $CD95^+$) $CD4^+$ T cells are poorly infected by HIV; while central memory T cells ($CD28^+$, $CD95^+$) are the primary cell type infected by HIV within the CD4 compartment (9). The latently infected pool of cells largely consist of central CD4+ memory T cells and transitional CD4+ memory T cells ($CD27^+$) (10, 11). The CD8 compartment isn't a primary source of viral

replication, but chronic inflammation drives hyperactivation and proliferation of these cells resulting in more terminally differentiated ($CD28^+$, $CD27^-$) effector CD8+ T cells. These terminally differentiated cells are less effective at controlling HIV replication and other opportunistic infections due to reduced replicative ability and cytotoxicity (12, 13).

Therapeutics that suppress viral replication and restore host immunological function hold the most potential for patient benefit. The CCR5 receptor antagonist Maraviroc is an approved cART drug and is effective in controlling HIV viral replication. CCR5 receptor antagonists have shown some efficacy at preventing cellular senescence in CD8+ T cells and reducing CD4+ and CD8+ T cell activation (HLA-DR+) in the blood (14). Some in vitro experiments have shown CCR5 antagonists to inhibit the chemotaxis of monocytes, macrophages, and dendritic cells; reducing dissemination of microbial pyogens systemically (15).

Due to ethical and technical challenges, data on the effects of Maraviroc therapy on organs such as lymph nodes is generally absent from the literature. The SIV/macaque model of HIV infection allows examination of aspects of disease that might be impractical in humans. These models have been reported to recapitulate many aspects of HIV disease including chronic inflammation associated with increased microbial translocation (16, 17). We used a rapidly progressing SIV/pigtailed macaque model of HIV to examine the effects of cART and cART plus Maraviroc (cART+M) on T cell expression of surface markers of memory and activation in the blood, intestinal mucosa, draining (colonic &

mesenteric) gut (GLN), and peripheral (axillary & inguinal) lymph nodes (PLN). This model exhibits a course of disease similar to SIV-infected rhesus macaques but in a compressed time span resulting in death around three months post inoculation, and can achieve viral suppression on cART therapy (18, 19, 20). The aim of the present study was to determine whether Maraviroc in addition to cART is more effective than cART alone at restoring the balance of T cell memory populations, reduces late stage differentiation of T cell memory populations, and reduces activation in tissues such as lymph nodes and gut.

Materials and Methods

Animal studies

Four cohorts of juvenile pigtailed macaques were used in this study. All infected groups were inoculated intravenously with two strains of SIV: the immunosuppressive swarm SIV/DeltaB670 and the neurovirulent clone SIV/17E-Fr, as previously described (18). Late stage infected (LSI) animals were euthanized at approximately 84 days post infection (p.i.). Procedural control (PC) animals were mock-infected, had blood sampled following the same experimental schedule as LSI animals and were euthanized at 84 days p.i. cART animals received a regimen containing the nucleotide reverse transcriptase inhibitors emtricitabine (FTC, Gilead) and tenofovir (PMPA, Gilead) at doses of 40 and 20 mg/kg SID SQ respectively, and the integrase inhibitor dolutegravir (GlaxoSmithKline) at a dose of 2.5 mg/kg SID SQ, beginning at 12 days after virus inoculation. cART+M animals received the same injectable drug regimen as cART animals as well as the CCR5 receptor antagonist Maraviroc (Pfizer, New York City, NY) at a dose of 20 mg BID PO.

cART and cART+M animals were monitored for viremia by quantitative real-time PCR (qRT-PCR) and experienced marked declines in plasma and CSF viral RNA levels, reaching <100 copy equivalents/mL by 50 days after treatment initiation. cART and cART+M animals were euthanized between 161-175 days post infection.

RNA extraction and viral RNA quantification

Viral RNA from jejunum, ileum, and colon was extracted from approximately 50 mg of frozen tissue using the RNeasy kit (Qiagen). Samples were eluted in 50 μL of water and analyzed by qRT-PCR for SIV RNA as described elsewhere (20). The limit of detection was established at 10 copies/reaction (100 copy equivalents/mL).

DNA extraction and viral DNA quantification

DNA from jejunum, ileum, and colon was extracted from approximately 50 mg of frozen tissue using the DNeasy kit (69504, Qiagen). Samples were eluted in 120 μL of water and analyzed by RT-PCR for SIV *gag* DNA and circular 2-LTRs as described elsewhere (21). Copy numbers were normalized to the single-copy cellular gene IFN-β.

Intestinal mucosa cell isolation

Tissue samples from the jejunum, terminal ileum, and distal colon were excised and placed in 50 mL conical vials containing cold RPMI 1640 (ThermoFisher) with 10% FBS (Atlanta Biologicals, Flowery Branch, GA). Each sample was trimmed to <1cm, opened longitudinally and washed three times in 45 mL of cold RPMI supplemented with HEPES (ThermoFisher) buffer. Samples were then placed in 7.5 mL of RPMI/HEPES containing 150 u/mL of collagenase type II (Worthington, Lakewood, NJ). The mucosa was separated from the remaining gut by scraping with a scalpel (Figure 2-1).

The mucosa was transferred to a gentleMACS C tube (Miltenyi, Bergisch Gladbach, Germany) containing another 7.5 mL of RPMI/HEPES/Collagenase (15 mL total). After 1 hour incubation on a rotisserie agitator at 37°C the samples were disrupted in a gentleMACS dissociator (Miltenyi) on the “Lung 2” setting. 15 mL of RPMI/HEPES containing 200 mM dithiothreitol (DTT) was added to the samples, which were passed through a 100 μm cell strainer (Corning, Corning, NY) and washed with 7.5 mL of RPMI/HEPES/DTT. Samples were then passed through a 40 μm cell strainer (Corning), washed with 7.5 mL of RPMI/HEPES/DTT and centrifuged for 10 minutes at 800 x g. The resulting pellets were washed twice with cold RPMI/HEPES and re-suspended in 10 mL of RPMI/HEPES for subsequent counting and staining.

Flow cytometry analysis

Cells (6×10^6) from gut mucosa were stained with fluorochrome-coupled antibodies (Figure 2-2A) for 20 minutes at room temperature (RT) and then fixed with 4% paraformaldehyde in PBS for 10 minutes at RT. Whole blood samples (100 μL) and cells (10^6) from lymph nodes were isolated as previously described (21) and stained with fluorochrome-coupled antibodies (Figure 2-2A) for 20 minutes at RT and fixed for 10 minutes with BD FACS Lysing Solution (Becton Dickinson, Franklin Lakes, NJ). All antibodies were tested for specificity using fluorescence minus one controls. After fixation, samples were analyzed using a BD LSR Fortessa cytometer and Diva software version 6.1.3 (Becton Dickinson).

FACS data were analyzed using FlowJo version 9.5.1. Representative gating schema are presented in Figure 2-2B.

Statistical analyses

Comparisons between multiple animal groups were made using Kruskal-Wallis tests followed by Dunn's multiple comparison tests between the mean ranks of every group. Comparisons between two groups were made using a Mann-Whitney test. Microsoft Excel 2013 was used to organize data. GraphPad Prism 6.0 was used to perform statistical analyses and generate graphs. Graphs showing Kruskal-Wallis group comparisons report *p* values after Dunn's correction.

Results

Viral RNA and DNA in gut mucosa

To evaluate viral replication and the size of the latent viral reservoir in the gut of treated animals, copies of SIV RNA per microgram of RNA; and copies of SIV DNA and circular 2-LTRs per million cells were quantitated using qRT-PCR and RT-PCR respectively. Compared to LSI animals, cART and cART+M groups experienced a four log reduction in the mean rank percentage for SIV RNA copies in the jejunum ($H = 6.694$, $p = 0.0370$), ileum ($H = 11.77$, $p = 0.0003$), and colon ($H = 11.77$, $p = 0.0003$), a two log reduction in the mean rank percentage for SIV DNA copies in the jejunum ($H = 7.357$, $p = 0.0147$), and colon ($H = 9.857$, $p = 0.0007$), and a one log reduction in the mean rank percentage for replicative circular-2LTRs in the jejunum ($H = 9.055$, $p = 0.0090$), and colon ($H = 7.261$, $p = 0.0184$). There was no significant difference in viral RNA, DNA, or circular-2LTRs between cART and cART+M groups (Figure 2-3).

CD4+ and CD8+ T cells in the blood, gut mucosa, and lymph nodes.

Flow cytometry was conducted to determine the percentage of $CD3^+$ T cells expressing CD4 or CD8. The mean rank percentage of $CD4^+$ T cells was significantly altered in the blood ($H = 7.985$, $p = 0.0463$), jejunum ($H = 13.630$ $p = 0.0035$), ileum ($H = 12.940$, $p = 0.0048$), and colon ($H = 11.60$, $p = 0.0089$). Percent of $CD4^+$ T cells were significantly lower in LSI animals compared to PC animals in the jejunum, ileum, and colon. cART animals had significantly higher percentages of $CD4^+$ T cells compared to LSI animals in the blood ($H = 7.985$, p

= 0.0290), jejunum (H = 13.63, p = <0.0001), and ileum (H = 12.94, p = 0.0002). The mean rank percentage of $CD8^+$ T cells was significantly altered in the blood (H = 9.052, p = 0.0286), and jejunum (H = 9.368, p = 0.0248). Percent of $CD8^+$ T cells were significantly lower in cART animals compared to LSI animals in the blood, and compared to cART+M animals in the jejunum. Dunn's p values for between-group comparisons are shown in Figure 1-4.

T cell memory populations by CD28 and CD95 expression

To assess the relative proportions of memory T cells, we examined the percentage of $CD4^+$ or $CD8^+$ T cells expressing $CD28/CD95^{+/-}$ (naïve), $CD28/CD95^{+/+}$ (central), or $CD28/CD95^{-/+}$ (effector). The mean rank percentage naïve $CD4^+$ T cells was significantly altered in the jejunum (H = 9.846, p = 0.0002), ileum (H = 7.269, p = 0.0159), colon (H = 6.000, p = 0.0403), and GLN (H = 7.636, p = 0.0038). Percent naïve $CD4^+$ T cells was significantly lower in cART animals compared to PC animals in the jejunum, ileum, and colon; and compared to cART+M animals in the GLN.

The mean rank for percentage central memory $CD4^+$ T cells was significantly altered in the jejunum (H = 7.565, p = 0.0094), ileum (H = 9.846, p = 0.0002), and colon (H = 8.769, p = 0.0012). Percent central memory $CD4^+$ T cells was significantly lower in cART animals compared to PC animals.

The mean rank for percentage effector memory $CD4^+$ T cells was significantly altered in the jejunum (H = 8.000, p = 0.0048), colon (H = 8.346, p = 0.0024), and GLN (H = 8.227, p = 0.0016). Percent effector memory $CD4^+$ T was

significantly lower in cART+M animals compared to PC animals in the jejunum, and colon; and cART animals compared to PC animals in the GLN. No differences between cART and cART+M animals were observed. Dunn's *p* values for between-group comparisons are shown in Figure 2-5A.

The mean rank for percentage naïve $CD8^+$ T cells was significantly altered in the jejunum (H = 9.846, *p* = 0.0002), ileum (H = 9.846, *p* = 0.0002), and colon (H = 7.731, *p* = 0.0066). Percent naïve $CD8^+$ T cells was significantly lower in cART animals compared to PC animals.

The mean rank for percentage central memory $CD8^+$ T cells was significantly altered in the jejunum (H = 7.385, *p* = 0.0145), ileum (H = 8.769, *p* = 0.0012), and colon (H = 7.731, *p* = 0.0066). Percent central memory $CD8^+$ T cells was significantly higher in cART animals compared to PC animals. No differences between cART and cART+M animals were observed. Dunn's *p* values for between-group comparisons can be found in Figure 2-5B.

T cell memory populations by CD27 expression

Memory populations were also analyzed by the percentage of $CD4^+$ or $CD8^+$ T cells expressing CD27 and the proportion of $CD4^+$ or $CD8^+$ naïve, central, or effector cells expressing CD27. The mean rank percentage of $CD4^+$ T cells expressing CD27 was significantly altered in the blood (H = 8.326, *p* = 0.0012), jejunum (H = 9.846, *p* = 0.0002), ileum (H = 9.846, *p* = 0.0002), colon (H = 8.115, *p* = 0.0031), GLN (H = 7.511, *p* = 0.0059), and PLN (H = 7.848, *p* =

0.0029). Percent of $CD4^+$ T cells expressing CD27 was significantly higher in cART+M animals compared to cART animals.

The mean rank percentage of $CD8^+$ T cells expressing CD27 was significantly altered in the ileum (H = 7.423, p = 0.0132), colon (H = 8.769, p = 0.0012). Percent of $CD8^+$ T cells expressing CD27 was significantly higher in cART+M animals compared to PC animals in the ileum and colon; and compared to cART animals in the ileum. Dunn's p values for between-group comparisons can be found in Figure 2-6A.

The median percentage of $CD4^+$ or $CD8^+$ naïve, central, or effector cells also expressing CD27 was significantly higher ($p < 0.05$) on all groups of memory T cells in cART+M animals in the gut mucosa compared to cART alone by Mann-Whitney U test. Excluding naïve $CD4^+$ T cells in the jejunum, all $CD8^+$ T cell memory populations in the jejunum, and naïve $CD8^+$ T cells in the ileum and colon (Figure 2-6B).

T cell memory activation assessed by CCR5, CCR7, and HLA-DR expression

To assess markers of T cells activation, the percentage of $CD4^+$ or $CD8^+$ T cells expressing CCR5, CCR7, or HLA-DR was measured. No significant differences in the mean rank percentages of $CD4^+$ T cells expressing CCR5 were observed. The mean rank percentage of $CD4^+$ T cells expressing CCR7 was significantly altered in the blood (H = 7.212, p = 0.0090). Percent $CD4^+$ T cells expressing CCR7 was significantly lower in cART+M compared to cART animals. The mean rank percentage of $CD4^+$ T cells expressing HLA-DR was significantly

altered in the jejunum (H = 8.028, p = 0.0042), ileum (H = 7.538, p = 0.0107), and colon (H = 6.962, p = 0.0194). Percent of $CD4^+$ T cells expressing HLA-DR was significantly lower in cART+M compared to cART animals. Dunn's p values for between-group comparisons are shown in Figure 2-7A.

The mean rank percentage of $CD8^+$ T cells expressing CCR5 was significantly altered in the PLN (H = 6.727, p = 0.0184). Percent $CD8^+$ T cells expressing CCR5 was significantly higher in cART+M animals compared to PC animals. The mean rank percentage $CD8^+$ T cells expressing CCR7 was significantly altered in the blood (H = 7.477, p =0.0062), GLN (H = 7.636, p = 0.0038), and PLN (H = 6.727 p = 0.0184). Percent $CD8^+$ T cells expressing CCR7 was significantly lower in cART+M compared to PC animals. The mean rank percentage $CD8^+$ T cells expressing HLA-DR was significantly altered in the jejunum (H = 6.615, p = 0.0242), ileum (H = 6.962, p = 0.0192), and colon (H = 7.565, p = 0.0092). Percent $CD8^+$ T cells expressing HLA-DR was significantly lower in cART+M compared to PC animals. Dunn's p values for between-group comparisons can be found in Figure 2-7B.

Discussion

Maraviroc has garnered interest as a potential immunomodulatory compound in addition to its ability to suppress HIV viral replication (22, 23). In this study, the addition of Maraviroc to cART resulted in significant alterations to both CD4+ and CD8+ T cell memory populations in the blood, lymph nodes, and especially the gut mucosa. Importantly, changes observed in the gut mucosa and lymph nodes were not consistently reflected in the blood and no changes in viral replication or reservoir size were observed.

Early depletion and lack of recovery of CD4+ T cell in the small intestine is one of the most cited features of HIV infection (1, 2). Our experiments recapitulated these findings in SIV-infected macaques treated with cART and cART+M, both of which failed to restore CD4+ T cells to PC levels in the jejunum. Interestingly, cART+M also failed to restore CD4+ T cell numbers to those of uninfected animals in the ileum, whereas cART alone was sufficient. This might be due to the unique nature of illeal peyers patches as dedicated antigen induction organs; a process that might be impaired by CCR5 antagonism; as has been demonstrated in rats and mice (24, 25).

We focused on CD95, CD28, and CD27 to differentiate classes of memory T cells, allowing us to infer memory status (naïve, central, and effector) and stage of differentiation (early, intermediate, late). Attempts to quantify and purge latently infected memory cells have principally focused on naïve, central, and transitional memory CD4+ T cells as they are the most productively infected by HIV (9, 10, 11). Our data shows an overall increased restoration of central

memory CD4+ and CD8+ T cells in the intestine in cART+M as compared with cART animals. This was accompanied by a reduction in the number of effector memory CD8+ T cells in the intestine. An increase in CD27 expression was observed in cART+M vs cART animals on CD4+ T cells in all areas of the body examined and on CD8+ T cells in the ileum and colon only. This increase in expression was seen on all memory populations (naïve, central, effector) excluding naïve CD4+ T cells in the jejunum, all memory CD8+ T cells in the jejunum, and naïve CD8+ T cells in the entire gut. These data together suggest that Maraviroc with cART is more effective at restoring naïve and central memory populations while reducing the amount of terminally differentiated memory T cells. Again, these shifts were not accompanied by any observable differences in viral replication or reservoir size measured by PCR. Importantly, these shifts were most robust in the intestinal mucosa and were not significantly reflected in the blood or PLN; sites most commonly sampled in human patients.

Restoration of memory T cell populations is a desirable goal in the treatment of patients as it should reduce abnormally high inflammation while allowing an effective adaptive immune response to pathogens (26, 27). A recent publication cites impairment of cART patients' CD4+ T cells' ability to up-regulate the co-stimulatory molecules CD28 and CD27 (28); phenomena that our data suggests could be reversible with Maraviroc. Further, we observed reduction in HLA-DR expression on both CD4+ and CD8+ T cells in the gut mucosa of cART+M as compared with cART animals. These changes were also not reflected in the blood, PLN or GLN. Also supporting the idea of reduced systemic

immunological activation and inflammation, cART+M animals had reduced levels of CCR7 expression on CD4+ T cells in the blood, and on CD8+ T cells in the blood, PLN, and GLN as compared to PC animals. Reduced CCR7 expression might indicate less lymph node trafficking occurring in response to antigen presentation or inflammatory cytokines by T cells (29, 30).

These data support the value of Maraviroc with cART as an immunomodulatory compound that might promote restoration of the adaptive immune system in patients. Immunological restoration has been attempted in patients with Maraviroc intensification with unsatisfactory results in regards to CD4+ T cell count and only mild improvement on central memory CD4+ T cell populations with observable reductions to activation via HLA-DR (31, 32). However, given our findings, these results might be due to patient sampling that was limited to the blood; especially given Maraviroc's propensity to accumulate in other tissues such as the gut.

Conversely, Maraviroc-induced immune restoration might be undesirable in shock and kill approaches to viral eradication. By increasing the naïve and central memory T cell pool and reducing its level of terminal differentiation Miraviroc might also increase the number of cells that are susceptible to infection by HIV (9, 10, 11). Further, infected memory T cell populations with lowered activation status might be less effectively targeted by HIV specific CD8+ T cells, a mechanism thought to be vital in the clearance of latently infected cells (33). Our data, however, did not support this idea as SIV DNA levels remained unchanged between cART and cART+M.

What remains unclear is the distribution of HIV infection in these altered memory T cell populations with Maraviroc treatment and how HIV specific CD8+ T cells might be affected by this therapy. Additionally, it would be interesting to determine how therapeutic intensification with Maraviroc compares to initiation of cART that includes Maraviroc from the start of antiretroviral therapy. Clinicians and researchers should be cautious about extending findings observed in the blood to other organs, especially the gut mucosa given our findings. While it might confound certain strategies of eradication, clearly Maraviroc holds promise as an immune-restorative cART regiment. Further investigation is needed in order to find where Maraviroc best fits into the arsenal of weapons medicine has against HIV.

Acknowledgements

Anti-retroviral drugs for macaques were generously donated by Gilead (tenofovir, emtricitabine), GlaxoSmithKline (dolutegravir), and Pfizer (Maraviroc). Special thanks to the excellent veterinary and animal care staff at Johns Hopkins University School of Medicine.

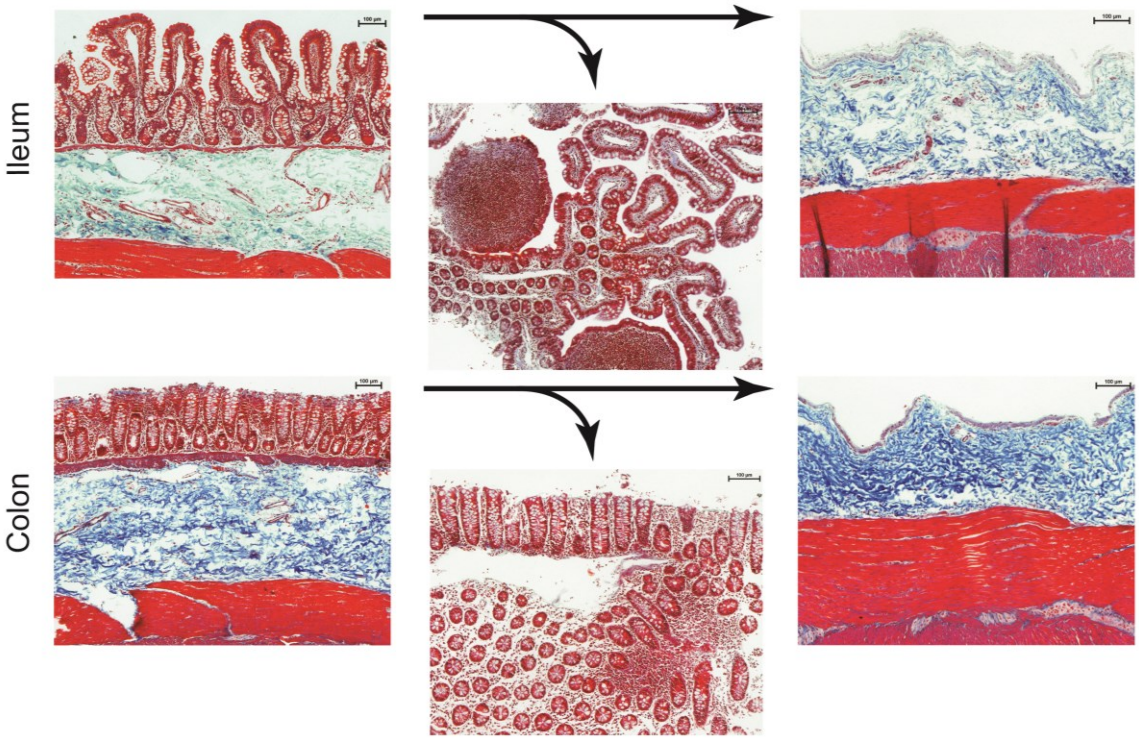

Figure 2-1. Isolation of gut mucosal cells.

A modified approach to isolating total cells from the lamina propria and epithelium of the gut. Mason's trichrome staining of tissue sections of ileum (top) and colon (bottom), showing full thickness gut before removal of musosa (left), mucosa after removal (middle) and the remaining gut (right).

A

Panel 1: Jejunum, ileum, colon

Target	Fluor	Clone	Company
CCR5	PerCP-Cy5.5	3A9	BD
CCR7	Pacific Blue	TG8	Biolegend
CD3	V500	SP34	BD
CD4	BV650	OKT4	Biolegend
CD8	BV570	RPA-T8	Biolegend
CD27	APC	M-T271	Biolegend
CD28	Alexa Fluor 700	CD28.2	Biolegend
CD95	PE	DX2	BD
HLADR	BV605	L234	Biolegend
Live/Dead	Aqua	L34965	ThermoFisher

Panel 2: Blood, GLN, PLN

Target	Fluor	Clone	Company
CCR5	PerCP-Cy5.5	3A9	BD
CCR7	Pacific Blue	TG8	Biolegend
CD3	FITC	SP34	BD
CD4	BV650	OKT4	Biolegend
CD8	BV570	RPA-T8	Biolegend
CD27	APC	M-T271	Biolegend
CD28	Alexa Fluor 700	CD28.2	Biolegend
CD95	PE	DX2	BD
HLADR	APC	L234	Biolegend

B

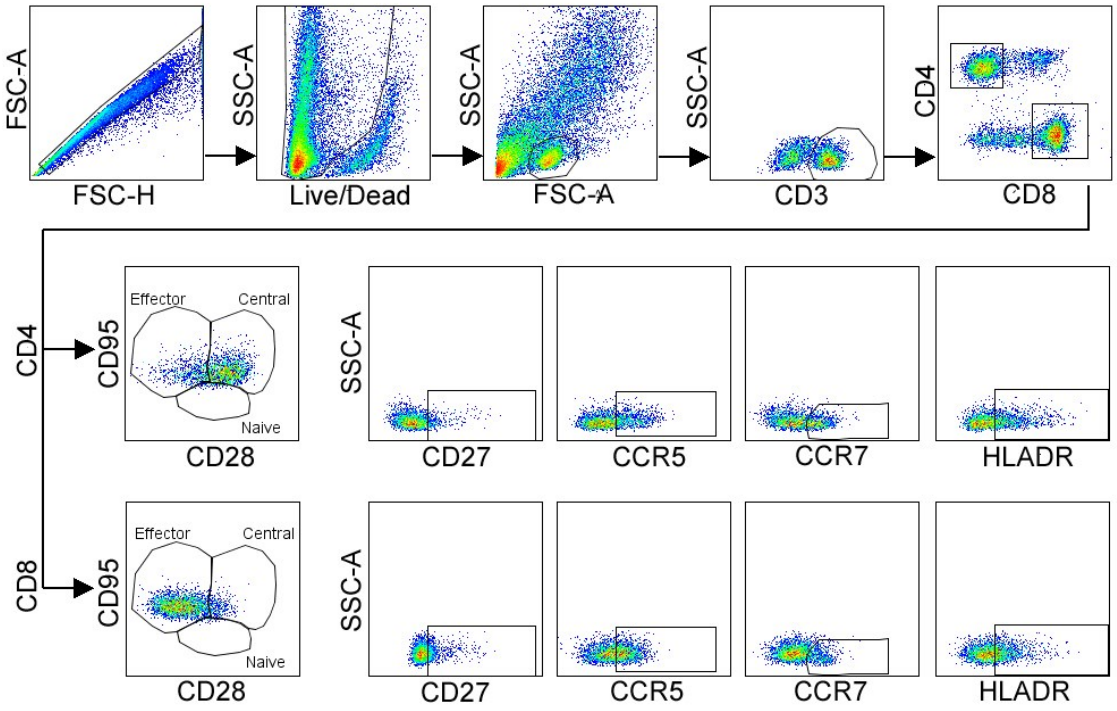

Figure 2-2. Flow cytometry analysis of blood, gut mucosa, and lymph nodes.

A modified approach to isolating total cells from the lamina propria and epithelium of the gut. **A)** Antibody panels used to label cells for flow cytometry. **B)** Gating schema used to analyze T cell populations.

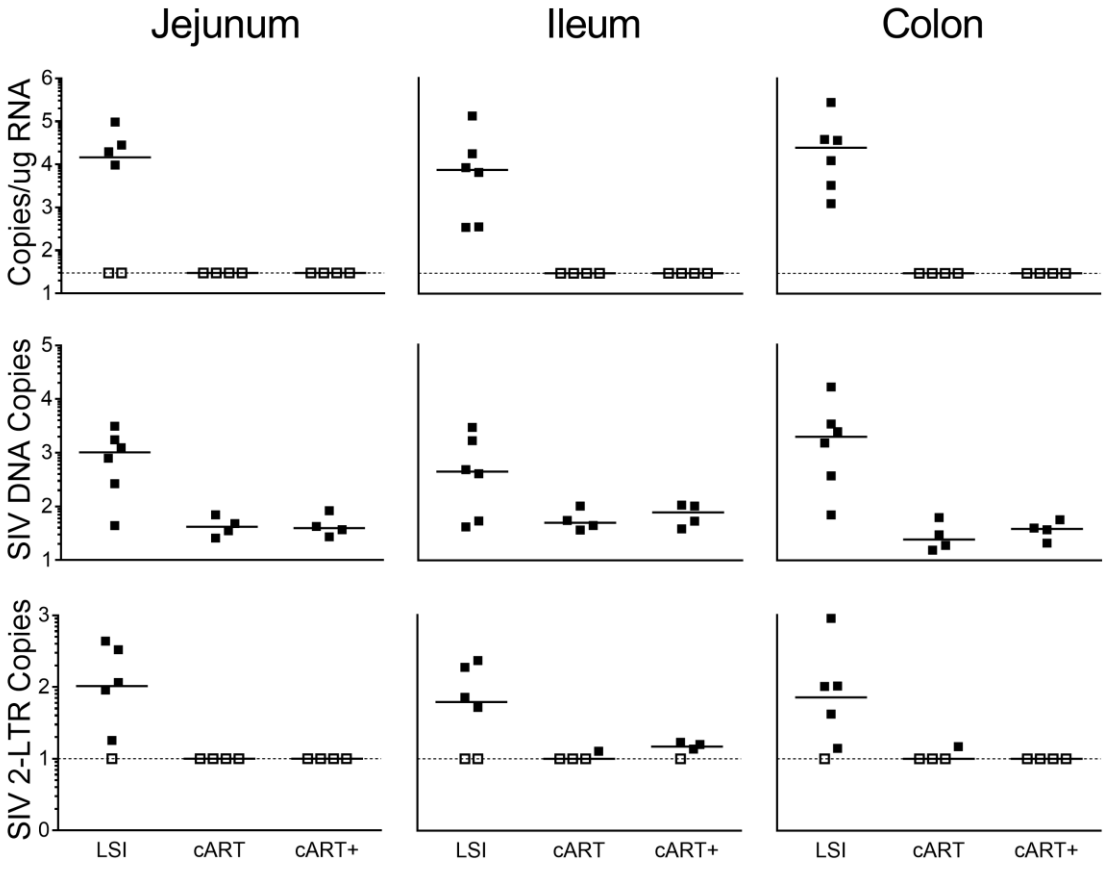

Figure 2-3. Viral RNA and DNA in the gut.

SIV RNA (top row), *gag* DNA (middle row), and circular 2-LTRs (bottom row) were measured by RT-PCR in the jejunum (left column), ileum (middle column), and colon (right column) of procedural control (PC) animals, animals on combination antiretroviral therapy (cART), and animals on combination antiretroviral therapy with Maraviroc (cART+M). Open squares represent samples that tested below the limit of sensitivity.

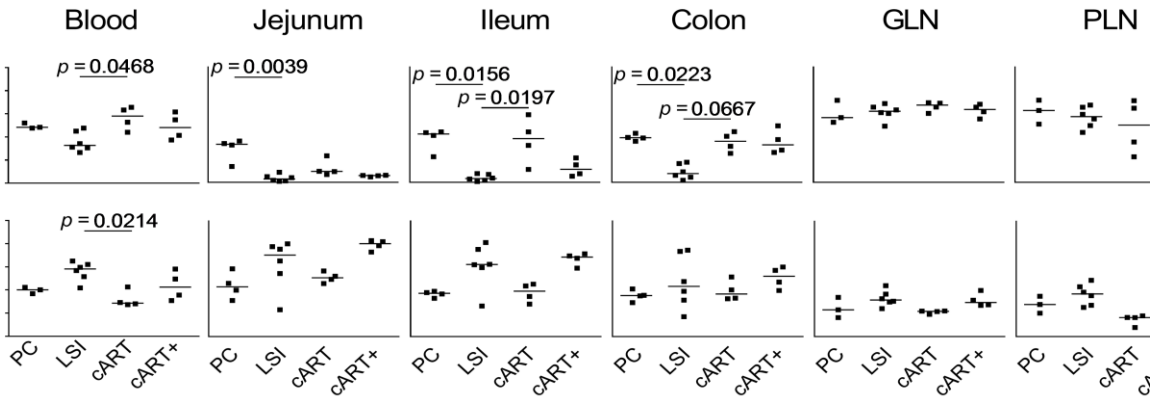

Figure 2-4. CD4+ and CD8+ T cell population alterations.

Samples from procedural control (PC) animals, late stage infected (LSI) animals, animals on combination antiretroviral therapy (cART), and animals on combination antiretroviral therapy that included Maraviroc (cART+M) were analyzed using flow cytometry for percentage of $CD3^+$ lymphocytes positive for CD4 (top row) or CD8 (bottom row) in the blood, gut, and lymph nodes. Lines represent group medians. Exact *p* values between groups were calculated by Kruskal-Wallis test followed by Dunn's post hoc correction.

Figure 2-5

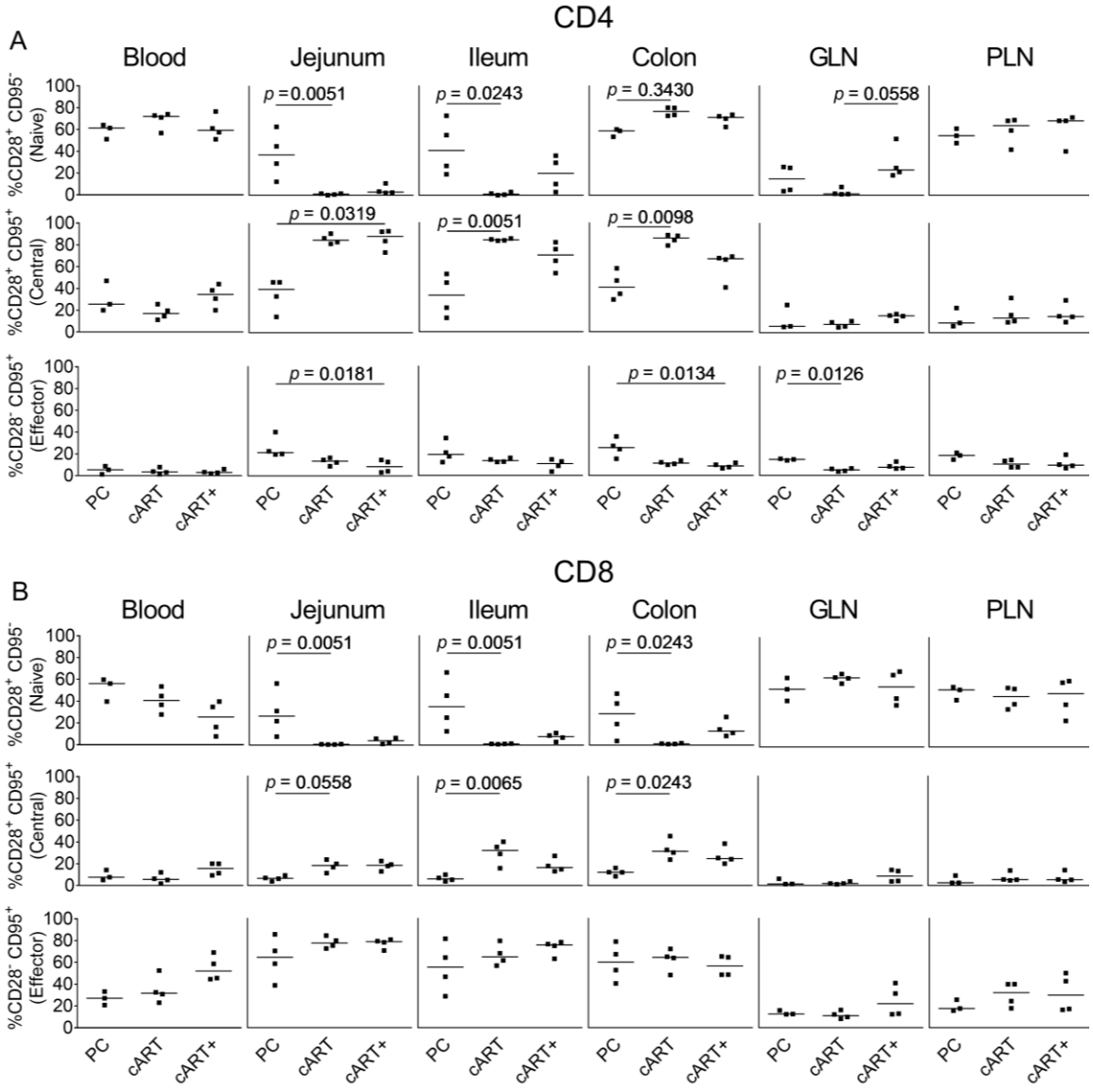
CD4
A
Blood
Jejunum
Ileum
Colon
GLN
PLN
%CD28+ CD95- (Naive)
%CD28+ CD95+ (Central)
%CD28- CD95+ (Effector)
p = 0.0051
p = 0.0243
p = 0.3430
p = 0.0558
p = 0.0319
p = 0.0051
p = 0.0098
p = 0.0181
p = 0.0134
p = 0.0126
PC
cART
cART+
CD8
B
Blood
Jejunum
Ileum
Colon
GLN
PLN
%CD28+ CD95- (Naive)
%CD28+ CD95+ (Central)
%CD28- CD95+ (Effector)
p = 0.0051
p = 0.0051
p = 0.0243
p = 0.0558
p = 0.0065
p = 0.0243
PC
cART
cART+

Figure 2-5. T cell memory population shifts examined by expression of CD28 and CD95.

Samples from procedural control (PC) animals, animals on combination antiretroviral therapy (cART), and animals on combination antiretroviral therapy that included Maraviroc (cART+M) were analyzed using flow cytometry for relative proportions of $CD4^+$ or $CD8^+$ T cells either $CD28/CD95^{+/-}$ (naïve memory), $CD28/CD95^{+/+}$ (central memory), $CD28/CD95^{-/+}$ (effector memory). **A)** $CD4^+$ T cell naïve memory (top row), central memory (middle row), or effector memory (bottom row) in the blood, gut mucosa, and lymph nodes. **B)** $CD8^+$ T cell naïve memory (top row), central memory (middle row), or effector memory (bottom row) in the blood, gut and lymph nodes. Lines represent group medians. Exact *p* values between groups were calculated by Kruskal-Wallis test followed by Dunn's post hoc correction.

Figure 2-6

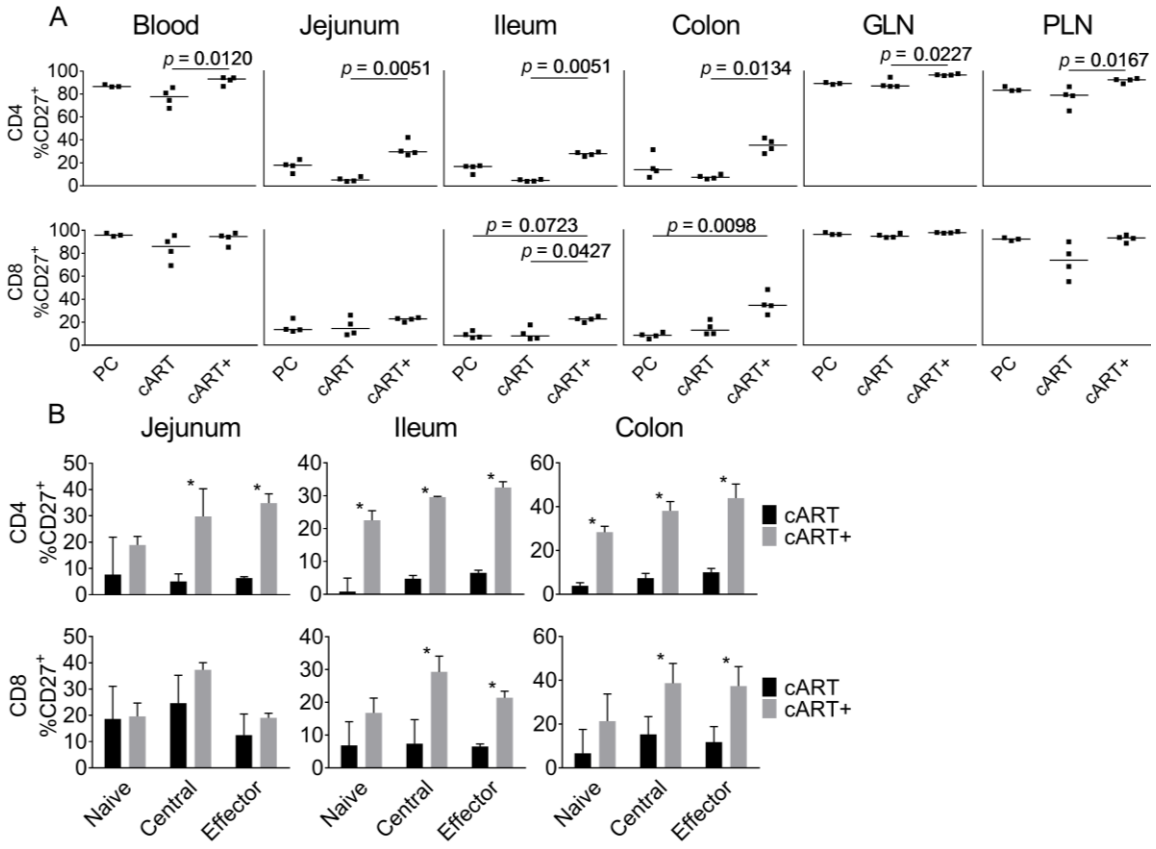
A
Blood
Jejunum
Ileum
Colon
GLN
PLN
p = 0.0120
p = 0.0051
p = 0.0051
p = 0.0134
p = 0.0227
p = 0.0167
p = 0.0723
p = 0.0427
p = 0.0098
CD4 %CD27+
CD8 %CD27+
PC
cART
cART+
B
Jejunum
Ileum
Colon
cART
cART+
Naive
Central
Effector

Figure 2-6. Distribution of CD27 expression on T cell memory subsets.

Samples from procedural control (PC) animals, animals on combination antiretroviral therapy (cART), and animals on combination antiretroviral therapy that included Maraviroc (cART+M) were analyzed using flow cytometry for relative proportions of $CD4^+$ or $CD8^+$ T cells positive for CD27. **A)** Percent of $CD4^+$ (top row) or $CD8^+$ (bottom row) T cells expressing CD27 in the blood, gut mucosa, and lymph nodes. Lines represent group medians. Exact *p* values between groups were calculated by Kruskal-Wallis test followed by Dunn's post hoc correction. **B)** Percent of $CD4^+$ (top row) or $CD8^+$ (bottom row) T cell memory populations (naïve, central, or effector) expressing CD27 in the blood, gut mucosa, and lymph nodes of animals on cART or cART & Maraviroc. Asterisks indicate mean ranks that were significantly different between indicated groups ($^*p < 0.05$) by Mann-Whitney Test.

Figure 2-7

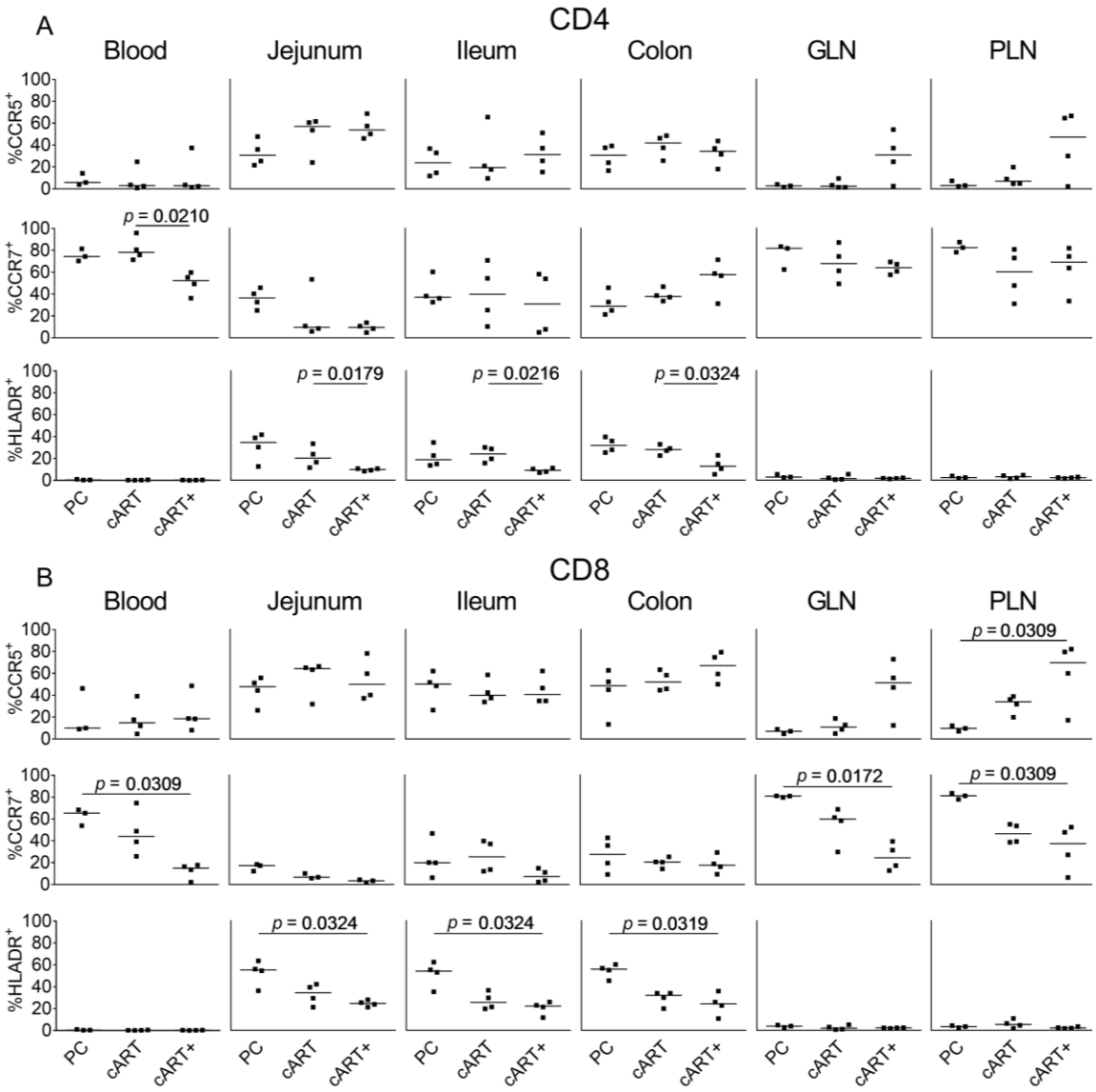
A
CD4
Blood
Jejunum
Ileum
Colon
GLN
PLN
%CCR5+
%CCR7+
%HLADR+
p = 0.0210
p = 0.0179
p = 0.0216
p = 0.0324
B
CD8
p = 0.0309
p = 0.0309
p = 0.0172
p = 0.0309
p = 0.0324
p = 0.0324
p = 0.0319
PC
cART
cART+

Figure 2-7. T cell activation evaluated by expression of CCR5, CCR7, and HLA-DR.

Samples from procedural control (PC) animals, animals on combination antiretroviral therapy (cART), and animals on combination antiretroviral therapy that included Maraviroc (cART+M) were analyzed using flow cytometry for relative proportions of $CD4^+$ or $CD8^+$ T cells positive for CCR5, CCR7, and HLA-DR. **A)** Percent of $CD4^+$ T cells expressing CCR5 (top row), CCR7 (middle row), or HLA-DR (bottom row) in the blood, gut mucosa, and lymph nodes. **B)** Percent of $CD8^+$ T cells expressing CCR5 (top row), CCR7 (middle row), or HLA-DR (bottom row) in the blood, gut mucosa, and lymph nodes. Lines represent group medians. Exact *p* values between groups were calculated by Kruskal-Wallis test followed by Dunn's post hoc correction.

CHAPTER IV.

Summary and Concluding Remarks

The findings presented in this dissertation are of key interest to researchers interested in HIV associated enteropathy and its relationship with the mucosal immune system, systemic inflammation, and microbial translocation. We examined a unique accelerated SIV model of HIV infection; thoroughly evaluating histopathological evidence of intestinal disease and found that, at least in this model, severe intestinal disease is not evident until late stage infection. This intestinal disease was highly associated with the number of CD3+ T cells in the mucosa of the ileum and colon. Additionally, these reductions in T cell staining were correlated with the amount of virally infected cells in the ileum and colon, plasma viral load, and apoptosis. The most significant findings from Chapter II were that while CD3+ T cells were indeed depleted during acute infection, as is often reported in HIV/SIV infection, there was no associated disruption of the epithelial barrier. Further, in animals with severe intestinal disease during chronic infection while there was disruption to the epithelial barrier, this did not correlate with increased microbial translocation as indicated by six different experiments measuring markers of translocation. We went on to demonstrate that cytotoxic T lymphocytes might play some role in preventing the development of intestinal disease.

As discussed in the Introduction, while intestinal disease and microbial translocation are often linked during HIV/SIV infection, the story is incomplete. The overall conclusion from this work is that microbial translocation does indeed occur during HIV/SIV infection, particularly during chronic, untreated infection. However, limitations of current methodologies for measuring microbial

translocation should be kept in mind and used to cautiously frame findings regarding microbial translocation; the findings in one experimental system or cohort of humans might have limited implications. Future studies regarding microbial translocation should incorporate our expanded understanding of the intestinal barrier and recent developments regarding the microbiota to refine the model for HIV/SIV associated inflammation. The intestinal barrier is maintained by a mucus layer, excreted antimicrobial peptides and IgA, epithelial tight junctions, and the mucosal immune system (1-3). Examination of one aspect of the intestinal barrier such as epithelial tight junctions might not be adequate to draw broad implications about the level of microbial translocation. Further, antigen induction can occur in the absence of intestinal barrier breakdown through the activities of dendritic cells and M-cells lining the luminal surface of the lamina propria.

Other potential sources of systemic inflammation might lie not in the induction or translocation of microbes and their antigens but in alterations to the microbiota species in the gut. A recent series of studies have linked specific bacteria taxa with alterations to tryptophan metabolism towards the pro-inflammatory kynurenine pathway (4); an inflammatory pathway that has been associated with inflammation in HIV (5, 6) and in the accelerated SIV macaque model of HIV disease (7). Additionally, some research has indicated that the presence of specific microbial taxa might increase recovery of CD4+ T cells and attenuate microbial translocation in the absence of cART, one example being increased proportions of Lactobacillales (8).

Expanding on the observation that intestinal disease in this model is highly associated with the number of CD3+ T cells and is prevented by cART; we sought to examine specific changes to T cell memory, differentiation status, and activation. One aspect of HIV/SIV cART that needs clarification is to what extent suppression of viral replication equates to immunological reconstitution. There is some evidence that initiation of cART during acute SIV infection in rhesus macaques might have a beneficial effect on correcting some immunological imbalances due to HIV infection (9). However, our findings indicated the opposite: initiation of cART at twelve days post infection was not sufficient to restore CD4+ and CD8+ T cell memory in the gut mucosa to proportions seen in uninfected animals; specifically with regards to numbers of naïve and central memory cells. Additionally, expression of CD27, a T cell co-stimulatory receptor that is lost on cells once they become exhausted in late stage differentiation, was lower on CD4+ T cells in every tissue examined, and on CD8+ T cells in the ileum and colon for animals receiving cART therapy. Together this indicates that the proportions of memory T cells are shifted and might be less able to appropriately and adaptively respond to antigen.

We next compared cART with cART including the CCR5 receptor antagonist Maraviroc. Maraviroc has garnered some attention in HIV therapeutics as a potential immunological modulatory agent as it interferes with accelerated chemotaxis of immunological cells towards sites of inflammation (10-12). We saw that cART+M was effective in restoring the proportions of CD4+ and CD8+ memory T cells towards those seen in uninfected animals over cART alone in the

intestinal mucosa. Most remarkably, expression of CD27 was markedly increased in all regions of the body examined compared to cART for CD4+ T cells and in the ileum and colon for CD8+ T cells. This increase in CD27 expression was seen on all types of CD4+ T cell memory (naïve, central, and effector) in the intestinal mucosa and on central and effector CD8+ memory T cells. This agrees with theories that Maraviroc holds therapeutic immunological benefit in the context of SIV disease. Restoration of the proportions of mucosal memory T cells in combination with a reduction in their exhaustion indicates the adaptive immune system is more able to respond appropriately and effectively in cART+M animals. This observation is further supported by our findings that markers of T cell activation were significantly lower in cART+M animals: CCR7 in the blood and lymph nodes (for CD8s) and HLA-DR in the gut mucosa for both CD4+ and CD8+ T cells.

Therapies that can effectively suppress viral replication and restore host immunity stand to greatly improve the quality of life of patients. A better understanding of how HIV/SIV can impact the intestinal immune system and possibly influence microbial translocation might offer novel therapeutic approaches that can be used in combination with cART and Maraviroc. Thus, important features of HIV and SIV infection that need clarification are the true quantity of microbial translocation occurring during infection and the amount of inflammation associated with changes in the microbiota that are independent of microbial translocation. This can be achieved with a combination of new technologies that allow researchers to more carefully examine microbially

sourced inflammation and thoughtful experimentation that keeps the complex physiology of the gut in mind. A revised model for systemic inflammation during HIV infection might allow clinicians to develop therapies that effectively silence most ailments experienced by HIV-infected individuals. Developing such a therapy in combination with highly effective antiretroviral agents stands to greatly benefit HIV-infected individuals by reducing inflammation and the incidence of non-AIDS related chronic illnesses. This and other strategies to reduce the incidence of chronic diseases experienced by HIV-infected individuals might one day eliminate the need for viral eradication from the host; a goal that has been sought for over three decades.

REFERENCES

Chapter I

1. Global summary of AIDS epidemic 2014. (2015, July 1). Retrieved January 11, 2016, from who.int website.
2. Lim, S.G., Condez, A., Lee, C.A., Johnson, M.A., Elia, C., and Poulter, L.W. 1993. Loss of mucosal CD4 lymphocytes is an early feature of HIV infection. Clinical & Experimental Immunology. 92, 3 (1993).
3. Brenchley, J., Schacker, T., Ruff, L., Price, D., Taylor, J., Beilman, G., Nguyen, P., Khoruts, A., Larson, M., Haase, A. and Douek, D. 2004. CD4+ T Cell Depletion during all Stages of HIV Disease Occurs Predominantly in the Gastrointestinal Tract. The Journal of Experimental Medicine. 200, 6 (2004), 749–759.
4. Palmer, S., Maldarelli, F., Wiegand, A., Bernstein, B., Hanna, G.J., Brun, S.C., Kempf, D.J., Mellors, J.W., Coffin, J.M. and King, M.S. 2008. Low-level viremia persists for at least 7 years in patients on suppressive antiretroviral therapy. Proceedings of the National Academy of Sciences of the United States of America. 105, 10 (Mar. 2008), 3879–84.
5. Maldarelli, F. et al. 2007. ART suppresses plasma HIV-1 RNA to a stable set point predicted by pretherapy viremia. PLoS pathogens. 3, 4 (Apr. 2007), e46.
6. Deeks SG, Lewin SR, Havlir DV. The end of AIDS: HIV infection as a chronic disease. Lancet 2013; 382(9903): 1525-33.

7. Boulware DR, Hullsiek KH, Puronen CE, et al. Higher levels of CRP, D-dimer, IL-6, and hyaluronic acid before initiation of antiretroviral therapy (ART) are associated with increased risk of AIDS or death.
8. Sereti, I. et al. 2016. Initiation of antiretroviral therapy in early HIV infection reduces but does not abrogate chronic residual inflammation. Clinical infectious diseases : an official publication of the Infectious Diseases Society of America. (Oct. 2016).
9. Marchetti, G., Bellistrì, G.M., Borghi, E., Tincati, C., Ferramosca, S., La Francesca, M., Morace, G., Gori, A. and Monforte, A.D. 2008. Microbial translocation is associated with sustained failure in CD4+ T-cell reconstitution in HIV-infected patients on long-term highly active antiretroviral therapy. AIDS (London, England). 22, 15 (Oct. 2008), 2035–8.
10. Sandler, N.G. et al. 2011. Plasma levels of soluble CD14 independently predict mortality in HIV infection. The Journal of infectious diseases. 203, 6 (Mar. 2011), 780–90.
11. Marchetti, G., Cozzi-Lepri, A., Merlini, E., Bellistrì, G.M., Castagna, A., Galli, M., Verucchi, G., Antinori, A., Costantini, A., Giacometti, A., di Caro, A. and D'arminio Monforte, A. 2011. Microbial translocation predicts disease progression of HIV-infected antiretroviral-naive patients with high CD4+ cell count. AIDS (London, England). 25, 11 (Jul. 2011), 1385–94.

12. Hunt, P.W. et al. 2014. Gut epithelial barrier dysfunction and innate immune activation predict mortality in treated HIV infection. The Journal of infectious diseases. 210, 8 (Oct. 2014), 1228–38.

13. Hunt, P.W., Landay, A.L., Sinclair, E., Martinson, J.A., Hatano, H., Emu, B., Norris, P.J., Busch, M.P., Martin, J.N., Brooks, C., McCune, J.M. and Deeks, S.G. 2011. A low T regulatory cell response may contribute to both viral control and generalized immune activation in HIV controllers. PloS one. 6, 1 (Jan. 2011), e15924.

14. Hunt PW, Brenchley J, Sinclair E, et al. Relationship between T cell activation and CD4+ T cell count in HIV-seropositive individuals with undetectable plasma HIV RNA levels in the absence of therapy

15. Knox, T., Spiegelman, D., Skinner, S. and Gorbach, S. 2000. Diarrhea and abnormalities of gastrointestinal function in a cohort of men and women with HIV infection. The American Journal of Gastroenterology. 95, 12 (2000).

16. Kotler, D.P. et al. Enteropathy associated with the acquired immunodefciency syndrome. Ann. Intern. Med. 101, 421–428 (1984)

17. Bhaijee, F., Subramony, C., Tang, S.-J. and Pepper, D. 2011. Human Immunodeficiency Virus-Associated Gastrointestinal Disease: Common Endoscopic Biopsy Diagnoses. Pathology Research International. 2011, (2011)

18. Lim, S.G., Condez, A., Lee, C.A., Johnson, M.A., Elia, C., and Poulter, L.W. 1993. Loss of mucosal CD4 lymphocytes is an early feature of HIV infection. Clinical & Experimental Immunology. 92, 3 (1993).

19. Brenchley, J., Schacker, T., Ruff, L., Price, D., Taylor, J., Beilman, G., Nguyen, P., Khoruts, A., Larson, M., Haase, A. and Douek, D. 2004. CD4+ T Cell Depletion during all Stages of HIV Disease Occurs Predominantly in the Gastrointestinal Tract. The Journal of Experimental Medicine. 200, 6 (2004), 749–759.

20. Guadalupe, M., Reay, E., Sankaran, S., Prindiville, T., Flamm, J., McNeil, A. and Dandekar, S. 2003. Severe CD4+ T-Cell Depletion in Gut Lymphoid Tissue during Primary Human Immunodeficiency Virus Type 1 Infection and Substantial Delay in Restoration following Highly Active Antiretroviral Therapy. Journal of Virology. 77, 21 (2003), 11708-11717.

21. Guadalupe, M., Sankaran, S., George, M., Reay, E., Verhoeven, D., Shacklett, B., Flamm, J., Wegelin, J., Prindiville, T. and Dandekar, S. 2006. Viral Suppression and Immune Restoration in the Gastrointestinal Mucosa of Human Immunodeficiency Virus Type 1-Infected Patients Initiating Therapy during Primary or Chronic Infection. Journal of Virology. 80, 16 (2006), 8236-8247.

22. Gazzola, L., Tincati, C., Bellistre, G., d'Arminio Monforte, A. and Marchetti, G. 2009. The Absence of CD4+ T Cell Count Recovery Despite Receipt of Virologically Suppressive Highly Active Antiretroviral Therapy: Clinical

Risk, Immunological Gaps, and Therapeutic Options. Clinical Infectious Diseases. 48, 3 (2009), 328-337.

23. Heise, C., Miller, C., Lackner, A. and Dandekar, S. 1994. Primary Acute Simian Immunodeficiency Virus Infection of Intestinal Lymphoid Tissue Is Associated with Gastrointestinal Dysfunction. Journal of Infectious Diseases. 169, 5 (1994), 1116-1120.

24. Gordon, S. et al. 2007. Severe Depletion of Mucosal CD4+ T Cells in AIDS-Free Simian Immunodeficiency Virus-Infected Sooty Mangabeys. The Journal of Immunology. 179, 5 (2007), 3026-3034.

25. Veazey, R., Tham, I., Mansfield, K., DeMaria, M., Forand, A., Shvetz, D., Chalifoux, L., Sehgal, P. and Lackner, A. 2000. Identifying the Target Cell in Primary Simian Immunodeficiency Virus (SIV) Infection: Highly Activated Memory CD4+ T Cells Are Rapidly Eliminated in Early SIV Infection In Vivo. Journal of Virology. 74, 1 (2000), 57-64.

26. Church, J. 2006. Massive Infection and Loss of Memory CD4+ T Cells in Multiple Tissues During Acute SIV Infection. PEDIATRICS. 118, Supplement_1 (2006), S52-S52.

27. Verhoeven, D., Sankaran, S., Silvey, M. and Dandekar, S. 2008. Antiviral Therapy during Primary Simian Immunodeficiency Virus Infection Fails To Prevent Acute Loss of CD4+ T Cells in Gut Mucosa but Enhances Their Rapid Restoration through Central Memory T Cells. Journal of Virology. 82, 8 (2008), 4016-4027.

28. Verhoeven, D., Sankaran, S. and Dandekar, S. 2007. Simian immunodeficiency virus infection induces severe loss of intestinal central memory T cells which impairs CD4+T-cell restoration during antiretroviral therapy. Journal of Medical Primatology. 36, 4-5 (2007), 219-227.

29. Inaba, K., Fukazawa, Y., Matsuda, K., Himeno, A., Matsuyama, M., Ibuki, K., Miura, Y., Koyanagi, Y., Nakajima, A., Blumberg, R., Takahashi, H., Hayami, M., Igarashi, T. and Miura, T. 2009. Small intestine CD4+ cell reduction and enteropathy in simian/human immunodeficiency virus KS661-infected rhesus macaques in the presence of low viral load. Journal of General Virology. 91, 3 (2009), 773-781.

30. Mattapallil JJ, Smit-McBride Z, Dailey P, Dandekar S. Activated Memory CD4+ T Helper Cells Repopulate the Intestine Early following Antiretroviral Therapy of Simian Immunodeficiency Virus-Infected Rhesus Macaques but Exhibit a Decreased Potential To Produce Interleukin-2. Journal of Virology. 1999;73(8):6661-6669.

31. Mattapallil JJ, Smit-McBride Z, McChesney M, Dandekar S. Intestinal Intraepithelial Lymphocytes Are Primed for Gamma Interferon and MIP-1β Expression and Display Antiviral Cytotoxic Activity despite Severe CD4+ T-Cell Depletion in Primary Simian Immunodeficiency Virus Infection. Journal of Virology. 1998;72(8):6421-6429.

32. Rallon, N., Sempere-Ortells, J., Soriano, V. and Benito, J. 2013. Central memory CD4 T cells are associated with incomplete restoration of the CD4 T cell pool after treatment-induced long-term undetectable HIV

viraemia. Journal of Antimicrobial Chemotherapy. 68, 11 (2013), 2616-2625.

33. Tanaskovic, S., Price, P., French, M. and Fernandez, S. 2016. Impaired upregulation of the costimulatory molecules CD27 and CD28 on CD4+ T-cells from HIV patients receiving ART is associated with poor proliferative responses. AIDS Research and Human Retroviruses. (2016).

34. Brenchley, J. et al. 2008. Differential Th17 CD4 T-cell depletion in pathogenic and nonpathogenic lentiviral infections. Blood. 112, 7 (2008), 2826-2835.

35. Cecchinato, V. et al. 2008. Altered balance between Th17 and Th1 cells at mucosal sites predicts AIDS progression in simian immunodeficiency virus-infected macaques. Mucosal Immunology. 1, 4 (2008), 279-288.

36. Klatt, Harris, Vinton, Sung, Briant, Tabb, Morcock, McGinty, Lifson, Lafont, Martin, Levine, Estes and Brenchley 2010. Compromised gastrointestinal integrity in pigtail macaques is associated with increased microbial translocation, immune activation, and IL-17 production in the absence of SIV infection. Mucosal immunology. 3, 4 (2010), 387–98.

37. Brenchley, J.M., Hill, B.J., Ambrozak, D.R., Price, D.A., Guenaga, F.J., Casazza, J.P., Kuruppu, J., Yazdani, J., Migueles, S.A., Connors, M., Roederer, M., Douek, D.C. and Koup, R.A. 2004. T-cell subsets that harbor human immunodeficiency virus (HIV) in vivo: implications for HIV pathogenesis. Journal of virology. 78, 3 (Feb. 2004), 1160–8

38. Farache, J., Zigmond, E., Shakhar, G. and Jung, S. 2013. Contributions of dendritic cells and macrophages to intestinal homeostasis and immune defense. Immunology and Cell Biology. 91, 3 (2013), 232–239.

39. Hoeffel, G. and Ginhoux, F. 2015. Ontogeny of Tissue-Resident Macrophages. Frontiers in immunology. 6, (Jan. 2015), 486.

40. Smythies, L., Sellers, M., Clements, R., Mosteller-Barnum, M., Meng, G., Benjamin, W., Orenstein, J. and Smith, P. 2005. Human intestinal macrophages display profound inflammatory anergy despite avid phagocytic and bacteriocidal activity. Journal of Clinical Investigation. 115, 1 (2005), 66–75.

41. Cassol, E., Rossouw, T., Malfeld, S., Mahasha, P., Slavik, T., Seebregts, C., Bond, R., du Plessis, J., Janssen, C., Roskams, T., Nevens, F., Alfano, M., Poli, G. and van der Merwe, S.W. 2015. CD14(+) macrophages that accumulate in the colon of African AIDS patients express pro-inflammatory cytokines and are responsive to lipopolysaccharide. BMC infectious diseases. 15, (Jan. 2015), 430.

42. Smith, P., Smythies, L., Shen, R., Greenwell-Wild, T., Gliozzi, M. and Wahl, S. 2010. Intestinal macrophages and response to microbial encroachment. Mucosal Immunology. 4, 1 (2010), 31-42.

43. Lim, S.G., Condez, A. and Poulter, L.W. 1993. Mucosal macrophage subsets of the gut in HIV: decrease in antigen-presenting cell phenotype. Clinical and experimental immunology. 92, 3 (Jun. 1993), 442–7.

44. Nazli, A., Chan, O., Dobson-Belaire, W.N., Ouellet, M., Tremblay, M.J., Gray-Owen, S.D., Arsenault, A.L. and Kaushic, C. 2010. Exposure to HIV-1 directly impairs mucosal epithelial barrier integrity allowing microbial translocation. PLoS pathogens. 6, 4 (Apr. 2010), e1000852.

45. Sereti, I. et al. 2016. Initiation of antiretroviral therapy in early HIV infection reduces but does not abrogate chronic residual inflammation. Clinical infectious diseases : an official publication of the Infectious Diseases Society of America. (Oct. 2016).

46. Abad-Fernández, M., Vallejo, A., Hernández-Novoa, B., Díaz, L., Gutiérrez, C., Madrid, N., Muñoz, M. and Moreno, S. 2013. Correlation between different methods to measure microbial translocation and its association with immune activation in long-term suppressed HIV-1-infected individuals. Journal of acquired immune deficiency syndromes (1999). 64, 2 (2013), 149–53.

47. Marchetti, G., Cozzi-Lepri, A., Merlini, E., Bellistrì, G.M., Castagna, A., Galli, M., Verucchi, G., Antinori, A., Costantini, A., Giacometti, A., di Caro, A. and D'arminio Monforte, A. 2011. Microbial translocation predicts disease progression of HIV-infected antiretroviral-naive patients with high CD4+ cell count. AIDS (London, England). 25, 11 (Jul. 2011), 1385–94.

48. Hunt, P.W. et al. 2014. Gut epithelial barrier dysfunction and innate immune activation predict mortality in treated HIV infection. The Journal of infectious diseases. 210, 8 (Oct. 2014), 1228–38.

49. Jiang, W., Lederman, M., Hunt, P., Sieg, S., Haley, K., Rodriguez, B., Landay, A., Martin, J., Sinclair, E., Asher, A., Deeks, S., Douek, D. and Brenchley, J. 2009. Plasma levels of bacterial DNA correlate with immune activation and the magnitude of immune restoration in persons with antiretroviral-treated HIV infection. The Journal of infectious diseases. 199, 8 (2009), 1177–85.

50. Balagopal, A., Gama, L., Franco, V., Russell, J.N., Quinn, J., Higgins, Y., Smeaton, L.M., Clements, J.E., Thomas, D.L. and Gupta, A. 2012. Detection of microbial translocation in HIV and SIV infection using the Limulus amebocyte lysate assay is masked by serum and plasma. PloS one. 7, 8 (Jan. 2012), e41258.

51. Ferri, E., Novati, S., Casiraghi, M., Sambri, V., Genco, F., Gulminetti, R. and Bandi, C. 2010. Plasma Levels of Bacterial DNA in HIV Infection: The Limits of Quantitative Polymerase Chain Reaction. The Journal of Infectious Diseases. 202, 1 (2010), 176-177.

52. Clements, J., Mankowski, J., Gama, L. and Zink, C. 2008. The accelerated simian immunodeficiency virus macaque model of human immunodeficiency virus–associated neurological disease: From mechanism to treatment. Journal of Neurovirology. 14, 4 (2008), 309–17.

53. Zink, M.C., Amedee, A.M., Mankowski, J.L., Craig, L., Didier, P., Carter, D.L., Muñoz, A., Murphey-Corb, M. and Clements, J.E. 1997. Pathogenesis of SIV encephalitis. Selection and replication of

neurovirulent SIV. The American journal of pathology. 151, 3 (Sep. 1997), 793–803.

54. Witwer, K.W., Gama, L., Li, M., Bartizal, C.M., Queen, S.E., Varrone, J.J., Brice, A.K., Graham, D.R., Tarwater, P.M., Mankowski, J.L., Zink, M.C. and Clements, J.E. 2009. Coordinated regulation of SIV replication and immune responses in the CNS. PloS one. 4, 12 (Jan. 2009), e8129.

55. Follstaedt, S.C., Barber, S.A. and Zink, M.C. 2008. Mechanisms of minocycline-induced suppression of simian immunodeficiency virus encephalitis: inhibition of apoptosis signal-regulating kinase 1. Journal of neurovirology. 14, 5 (Oct. 2008), 376–88.

56. Clements, J.E., Gama, L., Graham, D.R., Mankowski, J.L. and Zink, M.C. 2011. A simian immunodeficiency virus macaque model of highly active antiretroviral treatment: viral latency in the periphery and the central nervous system. Current opinion in HIV and AIDS. 6, 1 (Jan. 2011), 37–42.

Chapter II

1. Global summary of AIDS epidemic 2014 [Fact sheet]. (2015, July 1). Retrieved January 11, 2016, from who.int website.

2. Knox, T., Spiegelman, D., Skinner, S. and Gorbach, S. 2000. Diarrhea and abnormalities of gastrointestinal function in a cohort of men and women with HIV infection. The American Journal of Gastroenterology. 95, 12 (2000).

3. Kotler, D.P. et al. Enteropathy associated with the acquired immunodefciency syndrome. Ann. Intern. Med. 101, 421–428 (1984)

4. Bhaijee, F., Subramony, C., Tang, S.-J. and Pepper, D. 2011. Human Immunodeficiency Virus-Associated Gastrointestinal Disease: Common Endoscopic Biopsy Diagnoses. Pathology Research International. 2011, (2011)

5. Lim, S.G., Condez, A., Lee, C.A., Johnson, M.A., Elia, C., and Poulter, L.W. 1993. Loss of mucosal CD4 lymphocytes is an early feature of HIV infection. Clinical & Experimental Immunology. 92, 3 (1993).

6. Brenchley, J., Schacker, T., Ruff, L., Price, D., Taylor, J., Beilman, G., Nguyen, P., Khoruts, A., Larson, M., Haase, A. and Douek, D. 2004. CD4+ T Cell Depletion during all Stages of HIV Disease Occurs Predominantly in the Gastrointestinal Tract. The Journal of Experimental Medicine. 200, 6 (2004), 749–759.

7. Kanwar, B., Favre, D. and McCune, J. 2010. Th17 and regulatory T cells: implications for AIDS pathogenesis. Current Opinion in HIV and AIDS. 5, 2 (2010), 151.

8. Lim, S.G., Condez, A., and Poulter, L.W. 1993. Mucosal macrophage subsets of the gut in HIV: decrease in antigen-presenting cell phenotype. Clinical and experimental immunology. 92, 3 (1993).

9. Allers, K., Fehr, M., Conrad, K., Epple, H.-J., Schürmann, D., Geelhaar-Karsch, A., Schinnerling, K., Moos, V. and Schneider, T. 2013. Macrophages accumulate in the gut mucosa of untreated HIV-infected patients. The Journal of infectious diseases. 209, 5 (2013), 739–48.

10. Lehmann, C., Jung, N., Förster, K., Koch, N., Leifeld, L., Fischer, J., Mauss, S., Drebber, U., Steffen, H., Romerio, F., Fätkenheuer, G. and Hartmann, P. 2013. Longitudinal analysis of distribution and function of plasmacytoid dendritic cells in peripheral blood and gut mucosa of HIV-infected patients. The Journal of infectious diseases. 209, 6 (2013), 940–9.

11. Veazey, R.S., Rosenzweig, M., Shvetz, D.E., Pauley, D.R., DeMaria, M., Chalifoux, L.V., Johnson, R.P., and Lackner, A.A. 1997. Characterization of gut-associated lymphoid tissue (GALT) of normal rhesus macaques. Clinical immunology and immunopathology. 82, 3 (1997), 230–42.

12. Klatt, N.R., Harris, L.D., Vinton, C.L., Sung, H., Briant, J.A., Tabb, B., Morcock, D., McGinty, J.W., Lifsonm, J.D., Lafont, B.A., Martin, M.A., Levine, A.D., Estes, J.D., and Brenchley, J.M. 2010. Compromised gastrointestinal integrity in pigtail macaques is associated with increased microbial translocation, immune activation, and IL-17 production in the absence of SIV infection. Mucosal Immunology. 3, 4 (2010), 387–98.

13. Sandler, N. and Douek, D. 2012. Microbial translocation in HIV infection: causes, consequences and treatment opportunities. Nature Reviews Microbiology. 10, 9 (2012).

14. Estes, J. et al. 2010. Damaged Intestinal Epithelial Integrity Linked to Microbial Translocation in Pathogenic Simian Immunodeficiency Virus Infections. PLoS Pathogens. 6, 8 (2010), e1001052.

15. Jiang, W., Lederman, M., Hunt, P., Sieg, S., Haley, K., Rodriguez, B., Landay, A., Martin, J., Sinclair, E., Asher, A., Deeks, S., Douek, D. and Brenchley, J. 2009. Plasma Levels of Bacterial DNA Correlate with Immune Activation and the Magnitude of Immune Restoration in Persons with Antiretroviral-Treated HIV Infection. The Journal of Infectious Diseases. 199, 8 (2009), 1177–85.

16. Tincati, C., Douek, D. and Marchetti, G. 2016. Gut barrier structure, mucosal immunity and intestinal microbiota in the pathogenesis and treatment of HIV infection. AIDS Research and Therapy. 13, 1 (2016), 19.

17. Handley, S., Desai, C., Zhao, G., Droit, L., Monaco, C., Schroeder, A., Nkolola, J., Norman, M., Miller, A., Wang, D., Barouch, D. and Virgin, H. 2016. SIV Infection-Mediated Changes in Gastrointestinal Bacterial Microbiome and Virome Are Associated with Immunodeficiency and Prevented by Vaccination. Cell Host & Microbe. 19, 3 (2016), 323–335.

18. Clements, J., Mankowski, J., Gama, L. and Zink, C. 2008. The accelerated simian immunodeficiency virus macaque model of human

immunodeficiency virus–associated neurological disease: From mechanism to treatment. Journal of Neurovirology. 14, 4 (2008), 309–17.

19. Zink, M.C. and Clements, J. 2002. A Novel Simian Immunodeficiency Virus Model that Provides Insight into Mechanisms of Human Immunodeficiency Virus Central Nervous System Disease. Journal of Neurovirology. 8, 2 (2002), 42–48.

20. Zink, M.C., Brice, A.K., Kelly, K.M., Queen, S.E., Gama, L., Li, M., Adams, R.J., Bartizal, C., Varrone, J., Rabi, S.A., Graham, D.R., Tarwater, P.M., Mankowski, J.L. and Clements, J.E. 2010. Simian immunodeficiency virus-infected macaques treated with highly active antiretroviral therapy have reduced central nervous system viral replication and inflammation but persistence of viral DNA. The Journal of infectious diseases. 202, 1 (Jul. 2010), 161–70.

21. Zink, M.C., Uhrlaub, J., DeWitt, J., Voelker, T., Bullock, B., Mankowski, J., Tarwater, P., Clements, J. and Barber, S. 2005. Neuroprotective and Anti–Human Immunodeficiency Virus Activity of Minocycline. *JAMA*. 293, 16 (2005), 2003–2011.

22. Weed, M. R., R. D. Hienz, J. V. Brady, R. J. Adams, J. L. Mankowski, J. E. Clements, and M. C. Zink. 2003. Central nervous system correlates of behavioral deficits following simian immunodeficiency virus infection. J Neurovirol 9:452-464

23. Martin, L.N., Murphey-Corb, M., Soike, K.F., Davison-Fairburn, B., Baskin, G.B. 1993. Effects of initiation of 3'-azido,3'-deoxythymidine (zidovudine) treatment at different times after infection of rhesus monkeys with simian immunodeficiency virus. J Infect Dis. 168:825-835

24. Zeitz, M., Ullrich, R., Schneider, T., Kewenig, S., Hohloch, K., and Riecken, E.O. 1998. HIV/SIV Enteropathy. Annals of the New York Academy of Sciences. 859, 1 (1998)

25. Costiniuk, C., and Angel, J. 2012. Human immunodeficiency virus and the gastrointestinal immune system: does highly active antiretroviral therapy restore gut immunity? Mucosal Immunology. 5, 6 (2012), 596–604.

26. Smythies, L., Sellers, M., Clements, R., Mosteller-Barnum, M., Meng, G., Benjamin, W., Orenstein, J. and Smith, P. 2005. Human intestinal macrophages display profound inflammatory anergy despite avid phagocytic and bacteriocidal activity. Journal of Clinical Investigation. 115, 1 (2005), 66–75.

27. Smythies, L., Shen, R., Bimczok, D., Novak, L., Clements, R., Eckhoff, D., Bouchard, P., George, M., Hu, W., Dandekar, S. and Smith, P. 2010. Inflammation Anergy in Human Intestinal Macrophages Is Due to Smad-induced IκBα Expression and NF-κB Inactivation*. *The Journal of Biological Chemistry*. 285, 25 (2010), 19593–19604.

28. Cassol, E., Rossouw, T., Malfeld, S., Mahasha, P., Slavik, T., Seebregts, C., Bond, R., du Plessis, J., Janssen, C., Roskams, T., Nevens, F., Alfano,

M., Poli, G. and van der Merwe, S.W. 2015. CD14(+) macrophages that accumulate in the colon of African AIDS patients express pro-inflammatory cytokines and are responsive to lipopolysaccharide. BMC infectious diseases. 15, (Jan. 2015), 430.

29. Carter, C. and Ehrlich, L. 2008. Cell Biology of HIV-1 Infection of Macrophages. Annual Review of Microbiology. 62, 1 (2008), 425–443.

30. Williams, D.W., Engle, E.L., Shirk, E.N., Queen, S.E., Gama, L., Mankowski, J.L., Zink, M.C. and Clements, J.E. 2016. Splenic Damage during SIV Infection: Role of T-Cell Depletion and Macrophage Polarization and Infection. The American journal of pathology. (Jun. 2016).

31. Eugenin, E., Clements, J., Zink, M.C., and Berman, J. 2011. Human immunodeficiency virus infection of human astrocytes disrupts blood-brain barrier integrity by a gap junction-dependent mechanism. *The Journal of neuroscience : the official journal of the Society for Neuroscience*. 31, 26 (2011), 9456–65

32. Hoeffel, G. and Ginhoux, F. 2015. Ontogeny of Tissue-Resident Macrophages. *Frontiers in immunology*. 6, (Jan. 2015), 486.

33. Hasegawa, A., Liu, H., Ling, B., Borda, J.T., Alvarez, X., Sugimoto, C., Vinet-Oliphant, H., Kim, W.-K.K., Williams, K.C., Ribeiro, R.M., Lackner, A.A., Veazey, R.S. and Kuroda, M.J. 2009. The level of monocyte turnover predicts disease progression in the macaque model of AIDS. Blood. 114, 14 (Oct. 2009), 2917–25.

34. Abad-Fernández, M., Vallejo, A., Hernández-Novoa, B., Díaz, L., Gutiérrez, C., Madrid, N., Muñoz, M. and Moreno, S. 2013. Correlation between different methods to measure microbial translocation and its association with immune activation in long-term suppressed HIV-1-infected individuals. Journal of acquired immune deficiency syndromes (1999). 64, 2 (2013), 149–53.

35. Epple, H.-J.J., Allers, K., Tröger, H., Kühl, A., Erben, U., Fromm, M., Zeitz, M., Loddenkemper, C., Schulzke, J.-D.D. and Schneider, T. 2010. Acute HIV infection induces mucosal infiltration with CD4+ and CD8+ T cells, epithelial apoptosis, and a mucosal barrier defect. *Gastroenterology*. 139, 4 (Oct. 2010), 1289–300.

36. Epple, H.-J.J., Schneider, T., Troeger, H., Kunkel, D., Allers, K., Moos, V., Amasheh, M., Loddenkemper, C., Fromm, M., Zeitz, M. and Schulzke, J.-D.D. 2009. Impairment of the intestinal barrier is evident in untreated but absent in suppressively treated HIV-infected patients. *Gut*. 58, 2 (Feb. 2009), 220–7.

37. Luettig, J., Rosenthal, R., Barmeyer, C. and Schulzke, J.D. 2015. Claudin-2 as a mediator of leaky gut barrier during intestinal inflammation. Tissue barriers. 3, 1-2 (Jan. 2015), e977176.

38. Nazli, A., Chan, O., Dobson-Belaire, W.N., Ouellet, M., Tremblay, M.J., Gray-Owen, S.D., Arsenault, A.L. and Kaushic, C. 2010. Exposure to HIV-

1 directly impairs mucosal epithelial barrier integrity allowing microbial translocation. PLoS pathogens. 6, 4 (Apr. 2010), e1000852.

39. Epple, H.-J.J., Allers, K., Tröger, H., Kühl, A., Erben, U., Fromm, M., Zeitz, M., Loddenkemper, C., Schulzke, J.-D.D. and Schneider, T. 2010. Acute HIV infection induces mucosal infiltration with CD4+ and CD8+ T cells, epithelial apoptosis, and a mucosal barrier defect. Gastroenterology. 139, 4 (Oct. 2010), 1289–300.

40. Xu, H., Wang, X., Lackner, A.A. and Veazey, R.S. 2013. CD8 down-regulation and functional impairment of SIV-specific cytotoxic T lymphocytes in lymphoid and mucosal tissues during SIV infection. Journal of leukocyte biology. 93, 6 (Jun. 2013), 943–50.

41. Boichuk, S., Khaiboullina, S., Ramazanov, B., Khasanova, G., Ivanovskaya, K., Nizamutdinov, E., Sharafutdinov, M., Martynova, E., DeMeirleir, K., Hulstaert, J., Anokhin, V., Rizvanov, A. and Lombardi, V. 2015. Gut-Associated Plasmacytoid Dendritic Cells Display an Immature Phenotype and Upregulated Granzyme B in Subjects with HIV/AIDS. Frontiers in Immunology. 6, (2015), 485.

42. Dillon, S.M., Lee E.J., Kotter, C.V., Austin, G.L., Gianella, S., Siewe, B., Smith, D.M., Landay, A.L., McManus, M.C., Robertson, C.E., Frank, D.N., McCarter, M.D., and Wilson, C.C. 2016. Gut dendritic cell activation links an altered colonic microbiome to mucosal and systemic T-cell activation in untreated HIV-1 infection. Mucosal Immunology. 9, 1 (2016), 24–37.

43. Vujkovic-Cvijin, I., Dunham, R., Iwai, S., Maher, M., Albright, R., Broadhurst, M., Hernandez, R., Lederman, M., Huang, Y., Somsouk, M., Deeks, S., Hunt, P., Lynch, S. and McCune, J. 2013. Dysbiosis of the gut microbiota is associated with HIV disease progression and tryptophan catabolism. *Science translational medicine*. 5, 193 (2013), 193ra91.

44. Pérez-Santiago, J., Gianella, S., Massanella, M., Spina, C., Karris, M., Var, S., Patel, D., Jordan, P., Young, J., Little, S., Richman, D. and Smith, D. 2013. Gut Lactobacillales are associated with higher CD4 and less microbial translocation during HIV infection. *AIDS*. 27, 12 (2013), 1921.

Chapter III

1. Lim, S.G., Condez, A., Lee, C.A., Johnson, M.A., Elia, C., and Poulter, L.W. 1993. Loss of mucosal CD4 lymphocytes is an early feature of HIV infection. Clinical & Experimental Immunology. 92, 3 (1993).

2. Brenchley, J., Schacker, T., Ruff, L., Price, D., Taylor, J., Beilman, G., Nguyen, P., Khoruts, A., Larson, M., Haase, A. and Douek, D. 2004. CD4+ T Cell Depletion during all Stages of HIV Disease Occurs Predominantly in the Gastrointestinal Tract. The Journal of Experimental Medicine. 200, 6 (2004), 749–759.

3. Epple, H.-J.J., Allers, K., Tröger, H., Kühl, A., Erben, U., Fromm, M., Zeitz, M., Loddenkemper, C., Schulzke, J.-D.D. and Schneider, T. 2010. Acute HIV infection induces mucosal infiltration with CD4+ and CD8+ T cells,

epithelial apoptosis, and a mucosal barrier defect. Gastroenterology. 139, 4 (Oct. 2010), 1289–300.

4. Jiang, W., Lederman, M., Hunt, P., Sieg, S., Haley, K., Rodriguez, B., Landay, A., Martin, J., Sinclair, E., Asher, A., Deeks, S., Douek, D. and Brenchley, J. 2009. Plasma Levels of Bacterial DNA Correlate with Immune Activation and the Magnitude of Immune Restoration in Persons with Antiretroviral-Treated HIV Infection. The Journal of Infectious Diseases. 199, 8 (2009), 1177–85.

5. Sandler, N. and Douek, D. 2012. Microbial translocation in HIV infection: causes, consequences and treatment opportunities. Nature Reviews Microbiology. 10, 9 (2012).

6. Tincati, C., Douek, D. and Marchetti, G. 2016. Gut barrier structure, mucosal immunity and intestinal microbiota in the pathogenesis and treatment of HIV infection. AIDS Research and Therapy. 13, 1 (2016), 19.

7. Dillon, S.M., Lee E.J., Kotter, C.V., Austin, G.L., Gianella, S., Siewe, B., Smith, D.M., Landay, A.L., McManus, M.C., Robertson, C.E., Frank, D.N., McCarter, M.D., and Wilson, C.C. 2016. Gut dendritic cell activation links an altered colonic microbiome to mucosal and systemic T-cell activation in untreated HIV-1 infection. Mucosal Immunology. 9, 1 (2016), 24–37.

8. Cassol, E., Rossouw, T., Malfeld, S., Mahasha, P., Slavik, T., Seebregts, C., Bond, R., du Plessis, J., Janssen, C., Roskams, T., Nevens, F., Alfano, M., Poli, G. and van der Merwe, S.W. 2015. CD14(+) macrophages that

accumulate in the colon of African AIDS patients express pro-inflammatory cytokines and are responsive to lipopolysaccharide. BMC infectious diseases. 15, (Jan. 2015), 430.

9. Brenchley, J.M., Hill, B.J., Ambrozak, D.R., Price, D.A., Guenaga, F.J., Casazza, J.P., Kuruppu, J., Yazdani, J., Migueles, S.A., Connors, M., Roederer, M., Douek, D.C. and Koup, R.A. 2004. T-cell subsets that harbor human immunodeficiency virus (HIV) in vivo: implications for HIV pathogenesis. Journal of virology. 78, 3 (Feb. 2004), 1160–8

10. Chomont, N. et al. 2009. HIV reservoir size and persistence are driven by T cell survival and homeostatic proliferation. Nature medicine. 15, 8 (Aug. 2009), 893–900.

11. Zerbato, J.M., Serrao, E., Lenzi, G., Kim, B., Ambrose, Z., Watkins, S.C., Engelman, A.N. and Sluis-Cremer, N. 2016. Establishment and Reversal of HIV-1 Latency in Naive and Central Memory CD4+ T Cells In Vitro. Journal of virology. 90, 18 (Sep. 2016), 8059–73.

12. Papagno, L. et al. 2004. Immune activation and CD8+ T-cell differentiation towards senescence in HIV-1 infection. PLoS biology. 2, 2 (Feb. 2004), E20.

13. Chattopadhyay, P.K., Betts, M.R., Price, D.A., Gostick, E., Horton, H., Roederer, M. and De Rosa, S.C. 2009. The cytolytic enzymes granyzme A, granzyme B, and perforin: expression patterns, cell distribution, and

their relationship to cell maturity and bright CD57 expression. Journal of leukocyte biology. 85, 1 (Jan. 2009), 88–97.

14. Westrop, S.J., Moyle, G., Jackson, A., Nelson, M., Mandalia, S. and Imami, N. 2012. CCR5 antagonism impacts vaccination response and immune profile in HIV-1 infection. Molecular medicine (Cambridge, Mass.). 18, (Jan. 2012), 1240–8.

15. Rossi, R., Lichtner, M., De Rosa, A., Sauzullo, I., Mengoni, F., Massetti, A.P., Mastroianni, C.M. and Vullo, V. 2011. In vitro effect of anti-human immunodeficiency virus CCR5 antagonist Maraviroc on chemotactic activity of monocytes, macrophages and dendritic cells. Clinical and experimental immunology. 166, 2 (Nov. 2011), 184–90.

16. Veazey, R.S., Rosenzweig, M., Shvetz, D.E., Pauley, D.R., DeMaria, M., Chalifoux, L.V., Johnson, R.P., and Lackner, A.A. 1997. Characterization of gut-associated lymphoid tissue (GALT) of normal rhesus macaques. Clinical immunology and immunopathology. 82, 3 (1997), 230–42.

17. Klatt, N.R., Harris, L.D., Vinton, C.L., Sung, H., Briant, J.A., Tabb, B., Morcock, D., McGinty, J.W., Lifsonm, J.D., Lafont, B.A., Martin, M.A., Levine, A.D., Estes, J.D., and Brenchley, J.M. 2010. Compromised gastrointestinal integrity in pigtail macaques is associated with increased microbial translocation, immune activation, and IL-17 production in the absence of SIV infection. Mucosal Immunology. 3, 4 (2010), 387–98.

18. Clements, J., Mankowski, J., Gama, L. and Zink, C. 2008. The accelerated simian immunodeficiency virus macaque model of human immunodeficiency virus–associated neurological disease: From mechanism to treatment. Journal of Neurovirology. 14, 4 (2008), 309–17.

19. Zink, M.C. and Clements, J. 2002. A Novel Simian Immunodeficiency Virus Model that Provides Insight into Mechanisms of Human Immunodeficiency Virus Central Nervous System Disease. Journal of Neurovirology. 8, 2 (2002), 42–48.

20. Zink, M.C., Brice, A.K., Kelly, K.M., Queen, S.E., Gama, L., Li, M., Adams, R.J., Bartizal, C., Varrone, J., Rabi, S.A., Graham, D.R., Tarwater, P.M., Mankowski, J.L. and Clements, J.E. 2010. Simian immunodeficiency virus-infected macaques treated with highly active antiretroviral therapy have reduced central nervous system viral replication and inflammation but persistence of viral DNA. The Journal of infectious diseases. 202, 1 (Jul. 2010), 161–70.

21. Gama, L., Shirk, E.N., Russell, J.N., Carvalho, K.I., Li, M., Queen, S.E., Kalil, J., Zink, M.C., Clements, J.E. and Kallas, E.G. 2012. Expansion of a subset of CD14highCD16negCCR2low/neg monocytes functionally similar to myeloid-derived suppressor cells during SIV and HIV infection. Journal of leukocyte biology. 91, 5 (May 2012), 803–16

22. Wilkin, T.J. and Gulick, R.M. 2012. CCR5 antagonism in HIV infection: current concepts and future opportunities. Annual review of medicine. 63, (Jan. 2012), 81–93.

23. Woollard, S.M. and Kanmogne, G.D. 2015. Maraviroc: a review of its use in HIV infection and beyond. Drug design, development and therapy. 9, (Jan. 2015), 5447–68.

24. Pastori, C., Diomede, L., Venuti, A., Fisher, G., Jarvik, J., Bomsel, M., Sanvito, F. and Lopalco, L. 2014. Induction of HIV-blocking anti-CCR5 IgA in Peyers's patches without histopathological alterations. Journal of virology. 88, 7 (Apr. 2014), 3623–35.

25. Xu, H., Firdawes, S., Yamamoto, A., Zhao, Y., Ihara, Y., Uehara, S., Matsunami, K., Otsuka, H., Fukuzawa, M. and Miyagawa, S. 2008. Effects of Blocking the Chemokine Receptors, CCR5 and CXCR3, With TAK-779 in a Rat Small Intestinal Transplantation Model. Transplantation. 86, 12 (2008), 1810.

26. Rallón, N., Sempere-Ortells, J.M.M., Soriano, V. and Benito, J.M.M. 2013. Central memory CD4 T cells are associated with incomplete restoration of the CD4 T cell pool after treatment-induced long-term undetectable HIV viraemia. The Journal of antimicrobial chemotherapy. 68, 11 (Nov. 2013), 2616–25.

27. Corbeau, P. and Reynes, J. 2011. Immune reconstitution under antiretroviral therapy: the new challenge in HIV-1 infection. Blood. 117, 21 (May 2011), 5582–90.

28. Tanaskovic, S., Price, P., French, M. and Fernandez, S. 2016. Impaired upregulation of the costimulatory molecules CD27 and CD28 on CD4+ T-cells from HIV patients receiving ART is associated with poor proliferative responses. AIDS Research and Human Retroviruses. (2016).

29. Gómez, D., Diehl, M.C., Crosby, E.J., Weinkopff, T. and Debes, G.F. 2015. Effector T Cell Egress via Afferent Lymph Modulates Local Tissue Inflammation. Journal of immunology (Baltimore, Md. : 1950). 195, 8 (Oct. 2015), 3531–6.

30. Müller, G. and Lipp, M. 2003. Shaping up adaptive immunity: the impact of CCR7 and CXCR5 on lymphocyte trafficking. Microcirculation (New York, N.Y. : 1994). 10, 3-4 (Jun. 2003), 325–34.

31. Van Lelyveld, S.F. et al. 2015. Maraviroc Intensification of cART in Patients with Suboptimal Immunological Recovery: A 48-Week, Placebo-Controlled Randomized Trial. PloS one. 10, 7 (Jan. 2015), e0132430.

32. Gutiérrez, C. et al. 2011. Intensification of antiretroviral therapy with a CCR5 antagonist in patients with chronic HIV-1 infection: effect on T cells latently infected. PloS one. 6, 12 (Jan. 2011), e27864.

33. Deng, K. et al. 2015. Broad CTL response is required to clear latent HIV-1 due to dominance of escape mutations. Nature. 517, 7534 (Jan. 2015), 381–5.

Chapter IV

1. Camilleri, M., Madsen, K., Spiller, R., Van Meerveld, B. & Verne, G. Intestinal barrier function in health and gastrointestinal disease. Neurogastroenterology & Motility 24, 503-512 (2012).
2. Johansson MEV, Larsson JMH, Hansson GC. The two mucus layers of colon are organized by the MUC2 mucin, whereas the outer layer is a legislator of host–microbial interactions. Proceedings of the National Academy of Sciences of the United States of America. 2011;108(Suppl 1):4659-4665. doi:10.1073/pnas.1006451107.
3. Wells, J. & Mercenier, A. Mucosal delivery of therapeutic and prophylactic molecules using lactic acid bacteria. *Nature Reviews Microbiology* 6, 349-362 (2008).
4. Vujkovic-Cvijin, I., Dunham, R., Iwai, S., Maher, M., Albright, R., Broadhurst, M., Hernandez, R., Lederman, M., Huang, Y., Somsouk, M., Deeks, S., Hunt, P., Lynch, S. and McCune, J. 2013. Dysbiosis of the gut microbiota is associated with HIV disease progression and tryptophan catabolism. *Science translational medicine*. 5, 193 (2013), 193ra91.
5. Murray, M. Tryptophan depletion and HIV Tryptophan depletion and HIV infection: a metabolic link to pathogenesis. *The Lancet Infectious Diseases* 3, 644-652 (2003).

6. Potula R, Poluektova L, Knipe B, et al. Inhibition of indoleamine 2,3-dioxygenase (IDO) enhances elimination of virus-infected macrophages in an animal model of HIV-1 encephalitis. *Blood*. 2005;106(7):2382-2390. doi:10.1182/blood-2005-04-1403.

7. Drewes JL, Meulendyke KA, Liao Z, et al. Quinolinic acid/tryptophan ratios predict neurological disease in SIV-infected macaques and remain elevated in the brain under cART. *Journal of neurovirology*. 2015;21(4):449-463. doi:10.1007/s13365-015-0334-2.

8. Pérez-Santiago, J., Gianella, S., Massanella, M., Spina, C., Karris, M., Var, S., Patel, D., Jordan, P., Young, J., Little, S., Richman, D. and Smith, D. 2013. Gut Lactobacillales are associated with higher CD4 and less microbial translocation during HIV infection. *AIDS*. 27, 12 (2013), 1921.

9. Verhoeven, D., Sankaran, S., Silvey, M. and Dandekar, S. 2008. Antiviral Therapy during Primary Simian Immunodeficiency Virus Infection Fails To Prevent Acute Loss of CD4+ T Cells in Gut Mucosa but Enhances Their Rapid Restoration through Central Memory T Cells. Journal of Virology. 82, 8 (2008), 4016-4027.

10. Wilkin, T.J. and Gulick, R.M. 2012. CCR5 antagonism in HIV infection: current concepts and future opportunities. Annual review of medicine. 63, (Jan. 2012), 81–93.

11. Rossi, R., Lichtner, M., De Rosa, A., Sauzullo, I., Mengoni, F., Massetti, A.P., Mastroianni, C.M. and Vullo, V. 2011. In vitro effect of anti-human immunodeficiency virus CCR5 antagonist Maraviroc on chemotactic

activity of monocytes, macrophages and dendritic cells. Clinical and experimental immunology. 166, 2 (Nov. 2011), 184–90.

12. Gutiérrez, C. et al. 2011. Intensification of antiretroviral therapy with a CCR5 antagonist in patients with chronic HIV-1 infection: effect on T cells latently infected. PloS one. 6, 12 (Jan. 2011), e27864.

CURRICULUM VITAE

CURRICULUM VITAE

Joshua D. Croteau
2815 Echodale Ave.
Baltimore, MD 21214
301-639-3692 • J.Croteau87@gmail.com
Ph.D. Candidate at Johns Hopkins School of Medicine.

EDUCATION

Doctorate of Philosophy (Ph.D.) Expected Nov 2016

Johns Hopkins School of Medicine, Baltimore, MD

Program: Cellular and Molecular Medicine

Thesis Advisor: M. Christine Zink, DVM, PhD, ACV

Dissertation: Immunological enteropathy in an accelerated SIV macaque model of HIV disease.

Bachelors of Science in Physiology (B.S.) & Psychology (B.S.) June 2011

Towson University, Baltimore, MD

Honors: Honors in Biology, Cum Laude

Honors Thesis: Behavioral effects of chronically elevated corticosterone in subregions of the medial prefrontal cortex.

Honors & Awards: Chesapeake District Civitan International John Cain Scholarship, Lois D. Odell Scholarship for Outstanding Transfer Students

PROFESSIONAL EXPERIENCE

Ph.D. Candidate Researcher Aug 11 – Present

Johns Hopkins School of Medicine, Retrovirus Lab, Baltimore, MD

The retrovirus laboratory utilizes innovative animal models, including primates, to study infectious diseases in humans such as HIV.

- Designed and executed a large retroactive study of 15 years' worth of archival fluid and tissue samples.
- Collaborated on large multi-institutional study of macaques receiving antiretroviral therapy.
- Developed a unique and thorough scoring technique to quantify intestinal disease in animals.
- Profiled the dynamics of infected immunological cells in both fixed and live tissue samples.
- Linked pathological changes to the gut with unique gene expression profiles and surface protein changes.

- Examined the microbiota of animals and identified unique populations that impact SIV disease progression.
- Characterized the levels of active viral replication in gut and latent populations of virus.

Undergraduate Thesis Researcher Aug 10 – Aug 11'

Towson University, Neurobiology of Stress Laboratory, Baltimore, MD

- Conducted studies of the behavioral effects of glucocorticoids in animal models of physiological stress.
- Facilitated the success of other student's projects.

Research Assistant Aug 09 – Aug 10'

Towson University, Neurobiology of Stress Laboratory, Baltimore, MD

- Managed several animal cohorts utilized for multiple studies.
- Maintained the integrity of equipment and reagents utilized by lab members.

PUBLICATIONS

Meulendyke KA, **Croteau JD,** Zink MC., HIV life cycle, innate immunity and autophagy in the central nervous system. *Current Opinions in HIV & AIDS.* 9(6):565-571, November 2014.

Lucio Gama, Celina M Abreu, Erin N Shirk, Sarah L Price, Ming Li, Greg M Laird, Kelly A Metcalf Pate, Stephen W Wietgrefe, Shelby L O'Connor, Luiz Pianowski, Ashley T Haase, Carine Van Lint, Robert F Siliciano, **The LRA-SIV Study Group ψ,** Janice E Clements, Reactivation of SIV reservoirs in the brain of virally suppressed macaques, *AIDS (London, England). (Sep. 2016).*

Croteau, J.D., Schulkin, J. and Shepard, J.D. 2017. Behavioral effects of chronically elevated corticosterone in subregions of the medial prefrontal cortex. *Behavioral brain research*. 316, (Jan. 2017), 82–86.

Joshua D. Croteau, Elizabeth L. Engle, Erin Shirk, Suzanne Queen, M. Christine Zink, Marked enteropathy in an accelerated macaque model of AIDS. *American Journal of Pathology*, August 2016, *accepted.*

Drewes, J.L., **Croteau, J.,** Shirk, E., Engle, E., Zink, M.C., Graham, D.R. Maintenance of tissue tryptophan levels despite kynurenine pathway activation in SIV-infected pigtailed macaques, *Frontiers in Immunology,* September 2016*, accepted.*

Joshua D. Croteau, Erin Shirk, Ming Li, Joseph L. Mankowski, M. Christine Zink, Maraviroc with cART alters memory T cell

populations in the blood and organs of SIV infected, suppressed, pigtailed macaques. Journal of Infectious Disease, November 2016, *in preparation.*

Published Abstracts:

J. D. Croteau, J. Schulkin, J. D. Shepard, Behavioral effects of elevated corticosterone in the medial prefrontal cortex. Program No. 597.12/III23, San Diego CA: *Society for Neuroscience, 2010*

Joshua D. Croteau, M. Christine Zink, Marked enteropathy in an accelerated SIV model of HIV disease. Program No. , Boston MA, Keystone meeting for HIV persistence, *2015*

Presentations:

J. D. Croteau, J. Schulkin, J. D. Shepard, Behavioral effects of elevated corticosterone in the medial prefrontal cortex. Poster Presentation at the 40th annual scientific meeting of the Society for Neuroscience, San Diego, CA, *November 2010*

Joshua D. Croteau, M. Christine Zink, Marked enteropathy in an accelerated SIV model of HIV disease. Poster Presentation at Keystone meeting for HIV persistence, Boston, MA, *April 2015*

TECHNICAL EXPERTISE

Cellular & Molecular Biology: Multicolor flow cytometry and analysis, PCR (quantitative, digital droplet, real-time), ELISA, 16s rDNA sequencing and analysis, primary serological cell culture, Nanostring gene expression analysis, tissue dissociation and cellular isolation, BSL3 laboratory experience, RNA/DNA/MicroRNA isolation.

Histology and Pathology: Immunohistochemistry, in-situ hybridization, histopathological evaluation, cryo-sectioning, paraffin sectioning, histological fixation and differential staining.

Primate Models (BSL3): Drug administration, sample collection, necropsy.

Murine Models: Sterile survival surgery, stereotaxic surgery, anesthesia (Injection and Gas) and post-operative care, necropsy.

Murine Behavioral Testing: Elevated plus maze, forced swim test, open field test.

Software and Data Analysis: Microsoft Office (excel, word, powerpoint), Graphpad Prism, Adobe Photoshop, virtual machine emulation, R statistical analysis packages, Mothur 16s analysis.

TEACHING EXPERIENCE

Instructor May 2016 – Aug 16’

Johns Hopkins University, Baltimore, MD

Introductory Anatomy and Physiology, AS.020.375.11, Summer 2016

- Wrote and taught a series of lectures on the physiology and anatomy.
- Ensured the individual success of students through tutoring and advising.
- Evaluated mastery of lecture topics through exams and research papers.

Preparing Future Faculty Teaching Institute Summer 2014

Johns Hopkins School of Medicine, Week long intensive workshop series on active education and teaching as research in an undergraduate environment

Teaching Assistant Jan 2009 – Jun 11'

Stem-TC, Towson University, Introductory Biology

Academic Tutor Jan 2006 – Jun 11'

Towson University & Frederick Community College, General Chemistry 1 & 2, Human Anatomy & Physiology 1 & 2, Introductory Biology, Introductory Psychology

Mentoring:

Towson University:

Katie Kinsly, Graduate Student

Brittany Anderson, Undergraduate Student

Elliot Glotfelty, Undergraduate Student

Rachel Donahue, Undergraduate Student

Johns Hopkins University:

Roshni Banerjee, Summer CTY Student

Mary Soloman, Graduate Student

ORGANIZATIONAL EXPERIENCE

2009 – 2011 Beta Beta Beta Upsilon Eta, Biological Honors Society (Secretary, 2010)

2010 – 2011 Towson Energy Activists (Charter Member)

2010 – Present Society for Neuroscience, Member

2010 – Present American Physiological Society

2012 – Present American Society for the Advancement of Science